Characterization of the self-heat effect of thermistors in the VSL water calorimeter for absorbed dose

A study for accurate measurement methods using an Agilent 3458A opt. 002 digital multimeter

V.C.S. Hamoen

Delft, December 2013

A thesis in the partial fulfillment of the criteria for the BEng Applied Physics at The Hague University

Supervisors at The Hague University:
dr. L.H. Arntzen, drs. M.C. Vloemans

Supervisor at VSL:
L.A. de Prez MSc

Dutch Metrology Institute

VSL
Thijsseweg 11
2629 JA Delft
Postbus 654
2600 AR Delft
Nederland

T +31 15 269 15 00
F +31 15 261 29 71
E info@vsl.nl
I www.vsl.nl

This work has been carried out by:	V.C.S. Hamoen (11106263)
On request of:	L.A de Prez
For the applicant:	The Hague University, Technology, Innovation&Society Delft
Date	19-12-2013

Foreword

The past four months have been a lot. They were exciting, but sometimes boring. They were reinvigorating, but sometimes tiring. They were fast, but sometimes slow. They were an experience, always. Learning how to participate in a big project in a large company gave me hope. “Maybe this stuff isn’t so bad after all.” Except maybe the long hours.

Working at VSL was relieving. The colleagues were nice. The atmosphere in the company was good and the work was fun and challenging, most of the times. VSL is the Dutch metrology institute and it manages the national primary measurement standards. It is a unique company in the Netherlands with so many different fields of physics being driven to the edge of human capability. The Dutch kilogram and legal atomic time are kept and managed there, as are many other standards. It was an honor to be a part of something that significant and notable. The working life did not seem all that bad.

Working on this thesis has been educational, fun and had not been the same if it weren’t for my colleagues. With special thanks to: Helko van der Brom, for giving me insights in the workings of the Agilent 3458A digital multimeter and letting me lend his for an extended period of time. Bartel Jansen, for giving me feedback and was always ready to help me with almost anything, but especially the Delphi code. And of course, Leon de Prez. Not only a supervisor, but also a mentor. He always has been patient with me and was there when I needed him, providing me the nudges I needed to work towards an end goal.

Finally, some words of wisdom from one of earths’ greats. Words that I like to live by:

“If we knew what it was we were doing, it would not be called research, would it?”

-Albert Einstein-

Abstract

Research has been done to improve the understanding the self-heat effect, due to power dissipation, of temperature-dependant resistors in the VSL water calorimeter. A custom measurement program has been written to be able to control and read out three Agilent 3458A digital multimeters (DMMs). With these DMMs the course of resistance during the self-heating has been mapped and the timing of integration on this path has been determined. It was found that a Lauda cooling pump was inducing noise in the copper casing of the water calorimeter. This copper casing along with the DMMs have been grounded the same, which increased signal-to noise ratio by a factor 34.

Part of this analysis was the determination of the stability of the current provided by an Agilent 3458A DMM. The DCI mode (direct current) and the DCV mode (direct voltage) in combination with a shunt have been compared. The current measurement with the DCI mode resulted in 97.5334 μA ± 3.7 · 10^{-3} μA, with $k = 2$. The DCV-mode resulted in a current value of 97.5308 μA ± 3.3 · 10^{-3} μA, with $k = 2$, with standard deviations of 35 · μA/A for the DCI-mode and 11 μA/A for the DCV-mode. Which indicates the current to fluctuate within 1 nA in 68 % of the time when measuring in the 10 kΩ-range.

The two methods to measure the current stability have been compared using an EN-test. This test result yielded the value 0.53, which satisfies the set criterion of a value equal or smaller than two. This means the DCV-mode over a shunt method to measure current is accepted.

The DMMs provide several features to increase the accuracy of measurements. These features influence the measurement sequence and the measurement value. The OCOMP feature in particular was analyzed. This feature compensates for offsets and does so by comparing values with the measurement current enabled and disabled. This switching of the source current influences the terminal temperature of the self-heat greatly. An attempt has been made to fit this behavior to be able to estimate an effective power dissipation. The obtained curve was found to be an inadequate fit to the self-heating curve. A possible explanation for the lack of overlapping of these curves is that there is a steep temperature gradient in the water around the thermistor because of the stillness of the water.

The measurements for absorbed dose in water in the VSL water calorimeter are done with one OHMF-DMM measuring the resistance of the thermistor(s). To test, and possibly improve this method, the resistance is also measured with two DMMs measuring the voltage over the resistor separately. Two resistors R2 (20kΩ) and R3 (20kΩ) were connected parallel. The voltage over and current through these resistors was measured. The current was measured by using R1 (10kΩ) as a shunt, connecting it in series with the parallel resistors and measuring the voltage applied over it. The found values of the OHMF-method provided with a resistance value 9999.54 Ω ± 0.31 Ω, with $k = 2$. The two DCV-measuring DMMs provided a resistance value of 9997.35 Ω ± 0.35 Ω, with $k = 2$. The methods were compared using the EN-test. A test value of 4.7 was obtained, which violates the set criterion of the EN-test value equal or smaller than two. This rejects the method of measuring the resistance using two DCV-DMMs and a shunt. A plot of the measurement data shows that the method using two DMMs and a shunt is unstable and has an offset. The origin of these defects are unknown although previous results indicate that the defects are unlikely caused by instability in source current, but may originate from drift in shunt resistance and short aperture noise.

The measurement program was made to be able to control three DMMs and trigger them synchronously. The measurement data is plotted and printed in a table. Settings of the DMMs can be altered to change, including, but not limited to, their measurement function, integration time or sampling frequency. Several settings appeared to have a significant influence of the measurement results and need be set in a certain way or the program will not function properly.

DISP ON: Although this adds a delay, disabling the output to the display adds an unknown reading to the DCV-DMMs.

MEM FIFO: Disabling the reading memory returns the last readings made. With the used trigger set-up, this reading an AZERO reading. LIFO reversed the order of outputted data. This is not desired with continuous measurements.

OFORMAT DINT: Sets the output format to double integer values, the least data consuming format to retain full resolution.

END ALWAYS: Unlike ASCII, the DINT output format does not contain bits information of the line-feed and carriage-return. When using the DINT output format, this command ensures the individual readings are kept separated

TIMER: The TIMER command sets the time between the starts of two readings, which reciprocal is known as the sampling frequency. This has to be written as a decimal number.

APER: Sets the integration time of the ADC in seconds. The recommended maximum of this value is one tenth of the value set for TIMER with OCOMP and AZERO both on.

TARM AUTO: The commands that arms the trigger when the "TARM event" is satisfied. Sending single trigger arms in a loop to the OHMF-DMM prohibited the DCV-DMMs from making measurements.

Table of contents

1 Introduction

Radiotherapy is a widespread method for fighting malignant tumors. There have been major developments over the past decades concerning the accuracy of radiotherapy to limit the damage to the surrounding, healthy, tissue. There have been developments which, for example, led to the better molding of the shape of the irradiated area, the use of accelerators instead of a physical radiation source and an angle treatment where a lethal dose is deposited at the intersection of a number of beams

In all forms of radiotherapy the radiation sources have to be calibrated to verify that the selected amount of dose by the machine, or natural source, is, in fact, the absorbed dose by the tissue. Accelerators and X-ray radiation sources are configured with a calibrated secondary standard (ionization chamber) of the respective institute. These standards are calibrated at VSL with a primary standard and are provided with traceability to constants of nature. This primary standard is a so called water calorimeter (Kessler, Allisy-Roberts, de Prez, & de Pooter, 2009). Calorimeters are instruments used to measure energy. In this case the energy of a radiation source.

Primary standards for absorbed dose in water are usually graphite- or water calorimeters (BIPM). These calorimeters are irradiated whereby the temperature of the medium, water or graphite, rises. The advantage of water calorimeters is that they directly resemble human tissue. Graphite calorimeters are used because the heat capacity is several times lower than that of water and the temperature increases more with the same amount of incident radiation. The temperature rise due to the radiation is very small, but measurable. The VSL water calorimeter contains a water tank, which is thermally insulated from the outside and cooled using a regulating water cooler. This cooler circulates a mixture of alcohol and water through a tube system incorporated in the housing of the water tank. To uniformly dissipate the heat of the water, the pipes are attached to copper plates. Square holes in the copper plates minimize the scattering and absorption of the radiation beam.

Thermistors, which are temperature dependent resistors, are used for the measuring of the temperature change in the calorimeter. However, there are factors which impede on the accuracy of these measurements. Factors like impurities and turbulence in the water and the heating of the thermistors itself. This heating of the thermistors is caused by the current being driven through the thermistors, thus dissipating a power. Usually convective effects due to thermistor self-heating can be neglected because the order of magnitude of this effect is around 10 mK to 100 mK (de Prez, 2007 (revised 2008)), However, since the temperature increase due to the absorbed radiation is sub-mK, it is necessary to accurately characterize this self-heat effect in order to correct for it and to, ultimately, increase the accuracy of calibrations using the primary standard for absorbed dose in water of VSL.

There are several ways to characterize the thermistor self-heat effect in order to improve the accuracy of the correction of the self-heat effect. The following aspects have been investigated:

- Precise course of the resistance during the heating of the thermistors due to the source current.
- Optimizing the DMM measuring circuit with respect to signal to noise ratio and reduction of possible interference.
- Determination of the precise timing of the integration time on the heating curve.
- Determination of the effective dissipated power comparing a constant source current versus a square-wave source current
- The effects of variation in the settings of the digital multimeter used to measure the thermistors
- Confirming the resistance using three digital multimeters to validate both current and voltage.

The used methods can provide the total self-heat that can be used to correct for the self-heat in the water calorimeter for future as well as past measurements.

2 Theoretical background

In this chapter the relevant theoretical background of the water calorimeter and the thermistors as well as some fundamentals of the used digital multimeter will be discussed. The dimensions and some of the constants that are named are specifically for the water calorimeter at VSL.

2.1 Absorbed dose in water

To approximate the absorbed dose in human tissue, water is a very accurate substitute. A water calorimeter is a tank of demineralized water which can be placed in a beam of ionizing radiation. The water warms up by absorbing energy from the incident beam. By measuring the temperature increment of the water, the absorbed energy can be calculated with

$$E_a = m_w \cdot C_p \cdot \Delta T \tag{1}$$

With:

E_a	the absorbed energy by the water	[J]
m_w	the mass of the water absorbing the energy	[kg]
C_p	the specific heat capacity of water at constant pressure	[=4207.5 J/kg·K]
ΔT	the change in temperature of the water	[K]

This equation assumes the measured temperature is the applicable for the whole body of water at a certain depth. While irradiating the water, two temperature probes are placed equally distant from the center of the beam (at VSL at 0.5 cm). The water is kept very still and stable so that the flow of water is minimized and reduced to less than 0.5 μK·s^{-1} (de Prez, 2007 (revised 2008)) at normal circumstances. The exact mass of the irradiated body of water is irrelevant because the absorbed dose is a measure per mass. Equation (1) is rewritten to describe the absorbed dose in water:

$$D_w = C_p \cdot \Delta T \tag{2}$$

With:

D_w	the absorbed dose in water	[J/kg]

2.2 The self-heat effect

The before mentioned thermal probes are commonly called “thermistors”. This word is contracted from the words “thermal resistor”. Temperature dependent impedance of resistors is usually an unwanted effect in resistors. However, in thermistors, a strong change of the resistance as function of the temperature is beneficial for thermistors. The used thermistors are NTC thermistors. These are negative temperature coefficient semiconductors that decrease in resistance when the temperature rises. This is due to the fact that the electrons have higher thermal energy at higher temperatures, so more electrons reach the conduction band. As the conduction increases, the resistance decreases (Microchiptechnologies, 2010). The measure in which the resistance changes due to a change in temperature is also known as the sensitivity of the thermistor. Typical sensitivities of the VSL thermistors are 4.3 %/K (internal communication).

The self-heat effect is caused by the source current dissipating a power in the resistor, resulting in warming the thermistors itself and thus, the water surrounding it. This dissipation-energy rate is given by:

$$P = I^2 \cdot R \tag{3}$$

With:

P	the dissipated power in the resistor	[W]
I	the source current	[A]
R	the resistance of the thermistors	[Ω]

In some cases this effect can be exploited, but in accurate temperature change measurements, this effect causes an undesired variable offset several orders of magnitude larger than the temperature increment due to incident ionizing radiation.

The way the actual resistance of the thermistor changes due to the self-heat depends on the heat exchange processes of the thermistor with its surroundings. Once these are identified, the time-dependent self-heat effect can be described and ultimately corrected for.

2.3 Heat transfer

There are several ways for the thermistor to dissipate its thermal energy obtained by self-heating to the surrounding water i.e. radiation, convection and conduction. These effects describe the dissipation of the thermal energy to the water. The manner of energy dissipation by the thermistor isn't just important for the theoretical approximation of heat exchange between thermistor and water, but also for other physical transport phenomena induced in the rest of the water calorimeter. The different heat transfer effects are discussed separately for their individual influence on the problem.

2.3.1 Radiation

The Stefan-Boltzmann law describes how a blackbody radiator emits thermal energy depending on its temperature and that of its surroundings. The equation is given by (Giancoli, 2009)

$$\frac{P_R}{A} = \varepsilon \cdot \sigma \cdot T_o^4 \tag{4}$$

P_R	the emitted thermal energy by an object per second	[W]
A	the surface area of the radiating object	[m^2]
ε	the correction factor for non-ideal blackbody radiators	[-]
σ	the Stefan-Boltzmann constant	[=$5.670 \cdot 10^{-8}$ $W/m^2 \cdot K^4$]
T_o	the absolute temperature of the object	[K]

For non-ideal blackbody radiators in an environment that, itself, has temperature, the equation is slightly modified to:

$$P_R = \varepsilon \cdot \sigma \cdot A \cdot \left(T_o^4 - T_c^4 \right) \tag{5}$$

With:

T_c	the absolute temperature of the environment	[K]

Because the surface area of the thermistor probe (approximately 10^{-10} m^2) is very small, as is the temperature difference (up to 100 mK)(internal communication), the radiated thermal energy (approximately 10^{-30}W) is negligible. The typical energy received by the water calorimeter during a three minute run is about 1 Gy. The temperature difference of a one liter, spherical ideal black-body radiator has to be around 37 K for the power dissipated in the water due to the blackbody radiation to be about the same order of magnitude as the energy deposited in the water by the radiation source. Therefore it can be concluded that radiative heat transfer is negligible and all of the heat is dissipated through conduction and convection.

2.3.2 Convection

When the thermistor dissipates enough power, it can set in motion a flow in the water. This convection is a compromising factor in the stability of the water and thus in the homogeneity of the temperature of the irradiated volume. The density-curve of water reaches a minimum at approximately 4 °C. The slope of the density of this curve is zero at this point, which means that a small change in temperature will increase the density only by a small amount. For this reason, the water in the calorimeter is kept at 4 °C.

The effects of convection in the VSL water calorimeter have been analyzed and researched. It was found that the dissipated power, for $P < 0.12$ mW, is approximately proportional with ΔT, with a maximum uncertainty in ΔT of <2 mK (Cen, 2011). The highest dissipated power by the used measurement set-up has a value of 0.10 mW. Also, the conductive heat transfer coefficient has been analyzed using a model with- and without convection. The heat transfer coefficient without the effects of convection has been found to be 0.46 % lower than with convection. The heat transfer coefficient will be discussed extensively in the next paragraph.

2.3.3 Conduction

The above paragraphs showed that heat transfer from the thermistor to the water by radiation and convection can be neglected. The temperature change of the thermistor is completely due to the interaction between conduction of heat to the water and the heating of the thermistor itself. This interaction can be best described with an equation in differential form:

$$\frac{dE}{dt}_{inserted} = \frac{dE}{dt}_{absorbed} + \frac{dE}{dt}_{transferred} \tag{6}$$

With:

E	energy	[J]
t	time	[s]

As discussed before, the inserted energy is that which has been dissipated by the source current in the thermistor according to equation(3). The absorbed energy heats up the thermistor. The energy transferred from the thermistor to the water depends of a certain heat-transfer coefficient and the temperature difference between that of the water and the thermistor.

$$\frac{dE}{dt}_{transferred} = \delta \cdot \Delta T \tag{7}$$

With:

δ	heat-transfer coefficient of the thermistor	[W/K]
ΔT	temperature difference between the water and the thermistor	[K]

This heat-transfer coefficient depends on several variables like thermal conductivity in a certain medium, used materials in the probe as well as the geometry of the thermistor. This value has to be determined experimentally for every thermistor per specific medium (see Appendix II The determination of the heat-transfer coefficient, δ for the derivation).

The energy absorbed in the thermistor is described by:

$$\frac{dE}{dt}_{absorbed} = C_{Th} \cdot m \cdot \frac{d\Delta T}{dt} \tag{8}$$

With:

C_{Th}	the heat capacity of the thermistor	[J/kg·K]
m	the mass of the thermistor	[kg]

The last term of equation (8) describes the change in the temperature between the medium and the thermistor. This ΔT is equivalent to the self-heat of the thermistor. Combining equations (3), (7) and (8) gives the following expression:

$$P = \delta \cdot T_{SH} + C_{Th} \cdot m \frac{dT_{SH}}{dt} \tag{9}$$

With:

T_{SH}	the temperature increment due to the self-heat effect	[K]

Rewriting this equation yields

$$C_{Th} \cdot m \cdot \frac{dT}{dt} = P + \delta(\Delta T_{SH}) \tag{10}$$

This can be further rewritten as a differential in time, with ΔT_{SH} written as the water temperature, T_w minus the thermistor temperature, T_{Th}.

$$dt = \frac{C_{Th} \cdot m}{P + \delta(T_w - T_{Th})} dT_{Th} \tag{11}$$

With:

T_w	the temperature of the water	[K]
T_{Th}	the thermistor temperature	[K]

This equation can be integrated to obtain a solution to this equation, which is a time-dependent relation of the self-heat.

$$T(t) = C_1 e^{-\frac{\delta}{C_{Th} \cdot m} t} + \frac{P}{\delta} + T_w \tag{12}$$

With:

$$C_1 = \frac{P}{\delta} \tag{13}$$

Simplifying equation (12) and subtracting the term with the water temperature, T_w. provides with ΔT_{SH}

$$\Delta T_{SH}(t) = \frac{P}{\delta} \cdot \left(1 - e^{-\frac{\delta}{C_{Th} \cdot m} t} \right) \tag{14}$$

With:

$\Delta T_{SH}(t)$	the increment in temperature due to the self-heat effect as a function of time	[K]

When a constant source current is used and the system is in equilibrium (at $t \to \infty$), the complete exponential term is reduced to zero so that equation X is reduced to:

$$\Delta T_{SH} = \frac{I^2 \cdot R}{\delta} \tag{15}$$

The power dissipation is presumed to be constant in the above equations. However, this is proportional to the resistance of the resistor which the current is driven through. This resistance changes in time, because the temperature, and thus, the resistance changes in time.

2.3.4 Temperature dependent resistance

The thermistor resistance is not linear with a temperature increment, but this actually follows a logarithmic relation. As described by (Seuntjens, 1991). It is presumed that the resistance dependent of temperature is a first order relation. This means that *ln(R)* vs T^{-1} is a linear relation and yields:

$$R(T) = R_0 \cdot e^{\left(\beta \left(\frac{1}{T} - \frac{1}{T_0} \right) \right)} \tag{16}$$

With:

$R(T)$	the thermistor resistance as a function of temperature	[Ω]
R_0	the thermistor resistance without an applied current	[Ω]
β	a material constant	[K]
T	the absolute temperature of the thermistor	[K]
T_0	the absolute reference temperature	[K]

The above equation shows that the resistance is a function of temperature. Equation (14) was obtained by making the assumption that the power dissipated by the thermistor is constant. However, equation (16) states that the thermistor resistance, thus its power dissipation changes with temperature. Since the temperature changes in time, an expression can be made for the self-heat temperature as function of time including a time-dependent function for dissipated power

$$dt = \frac{C_{Th} \cdot m}{P(t) + \delta(T_w - T_{Th})} dT_{Th} \tag{17}$$

Solving this differential equation provides with a complex function, which cannot easily be plotted. To be able to plot this curve, the differential equation (9) can be rewritten to a discrete equation

DISP ON: Although this adds a delay to the measurement sequence, it prevents an unknown extra reading to appear in the first measurement.

MEM FIFO: This outputs the data chronologically. MEM LIFO outputs the readings of a measurement in reversed order. Which in inconvenient in continuous measurements, and MEM OFF outputs only the last value. In the used triggering settings, this value is the AZERO reading with source current disabled, which holds no useful information.

OFORMAT DINT: Output the data in the double integer format. This format requires the least amount of bits, while retaining maximum resolution.

END OFF: Unlike ASCII, the output format DINT does not contain its own line-feed or carriage-return bits. This command ensures the readings are kept separate.

NRDGS, EVENT: Sets the number of readings that will be made once the trigger is armed and the trigger event is satisfied. Possible events include, but are not limited to: "EXT", the EXT TRIG input, "AUTO", as soon as the controller requests data or "TIMER", with a specified time interval between the start of two readings.

TARM: During initialization the trigger is unarmed, or on "hold". The DMMs can be initialized and will wait until both the trigger arm event, as the trigger events are satisfied. Clicking the "Measure drift" button sends the trigger arm command and the DMM starts measuring as soon as the trigger arm- and the trigger events are satisfied. Giving the OHMF-DMM a single trigger arm was considered. When each DMM is read out, the OHMF-DMM would receive another single trigger. This makes the speed of the program direct how fast the measurements are done. It was believed the measurement program would not be fast enough to process all the data and slowing the measurement sequence down to the speed of the program could be beneficial. However, the system with the single triggers somehow caused the DCV-DMMs to not do any readings.

$$\frac{dT_{SH}}{dt} \approx \frac{T_n - T_{n-1}}{t_n - t_{n-1}} = P + \frac{\delta}{m \cdot C_{Th}} \cdot \frac{T_0 - T_{n-1}}{t_n - t_{n-1}} \tag{18}$$

With:

T_n	the thermistor temperature at *n*	[K]
t_n	the time at *n*	[s]
T_0	the thermistor temperature at *n=0*	[K]

This equation assumes constant power dissipation. The power dissipation as a function of time can be given by a combination of equation (3) and (16). Rewriting equation (18) to

$$\frac{T_n - T_{n-1}}{t_n - t_{n-1}} = I^2 \cdot R_0 \cdot e^{\left(\beta \cdot \left(\frac{1}{T_n} - \frac{1}{T_0}\right)\right)} + \frac{\delta}{m \cdot C_{Th}} \cdot \frac{T_0 - T_{n-1}}{t_n - t_{n-1}} \tag{19}$$

2.4 Digitizing with Agilent 3458A

The used digital multimeters are two Agilent 3458A, option 002 and one (older) HP 3458A option 002 DMM. These multimeters are highly accurate and are common in metrology labs throughout the world. Because of the minimal increment in temperature of the thermistor due to the incident radiation (approx. 0.24 mK/Gy), the change in resistance is also very small. Using the approximation of 430 Ω/K and the small temperature rise of 0.24 mK results in a change in resistance of approximately 100 mΩ. With a 10 kΩ resistor, that means a change in the sixth digit of the instrument. The Agilent/HP 3458A is a multimeter capable of measuring that small difference with precision.

2.4.1 Digitizing

The Agilent 3458A digital multimeter (hereby sometimes referred to as "DMM") is capable of exchanging information through the use of GPIB interface. This is an interface commonly used by producers of laboratory equipment to accommodate digital data acquisition through the use of a personal computer. A GPIB adapter can be connected to a computer using the National Instruments GPIB USB controller. Multiple program compilers are capable of controlling the GPIB devices using an interface like Delphi or LabVIEW. For most compilers, a library has to be programmed first to correctly interpret the data provided by the DMM. During this thesis, Delphi has been used as a compiler for the sake of compatibility, as most of the programs at VSL are written in Delphi and may be used to exchange code.

Digitizing the measurement results is done by sending the DMM a number of initialization settings depending of the desired measurement along with an arming signal. When the DMM is armed, it will start measuring upon satisfaction of the trigger event. The multimeter saves a number of measurements in its reading memory (if it is switched on) and then outputs it on request through the GPIB interface to the measurement computer. General settings sent to the DMM include, but are not limited to: integration time, measurement function and range, sample frequency, compensation internal or external offsets, trigger event and arming event. The most important functions/settings will be discussed later in this chapter.

2.4.2 OHMF- and DCV-modes

The measurement mode used for making resistance measurements can be either the "OHM"- or the "OHMF"-mode. The former makes two-wire resistance measurements, the latter four-wire resistance measurements. Four-wire measurements are more accurate because wires (=leads) that measure the voltage, are parallel to those that carry the current. Figure 1 shows the circuit diagram of an Agilent 3458A measuring resistance, using the four-wire method.

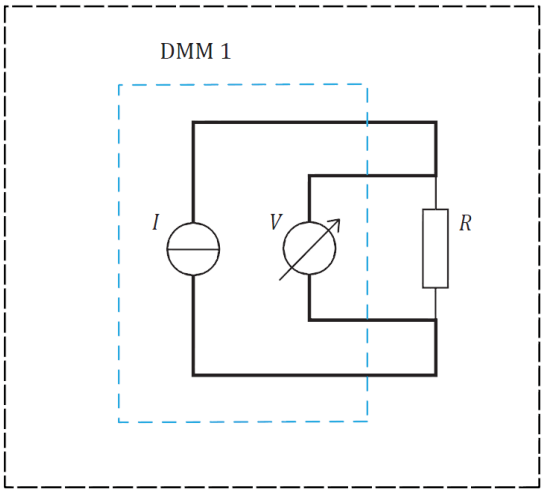

Figure 1 Circuit diagram of an Agilent 3458A performing an OHMF-measurement

The voltage measured is a sum of the voltage over the unknown resistor and that of the leads. Voltage is the product of resistance and current. In the four-wire method, the voltage is measured parallel to the current source over the unknown resistor. Because a voltmeter has high input impedance and is connected parallel to the unknown resistor, the current through, and thus the voltage across, the voltage measurement leads in the four-wire method is negligible.

During these measurements, the DMM itself provides the source current while it measured the applied voltage. The "DCV"-mode of the DMM (for direct voltage measurements) is the most accurate mode of this

particular DMM. Its most accurate range is the 1 V range. Therefore, during the resistance measurements, the current driven through the resistor is chosen so by the DMM, that the applied voltage is best measurable in the 1 V range.

2.4.3 Influences of OCOMP and AZERO setting

The OCOMP function is a useful tool of the Agilent 3458A for resistance measurements. OCOMP stands for offset compensated ohms. This function measures the input voltage during a 2- or 4-wire resistance measurement and then measures the input voltage again, but this time the source current has been disabled. The true induced voltage over the resistor is the difference between both readings. This function doubles the time needed for a measurement.

The AZERO function is similar to the OCOMP function. AZERO stands for auto-zero. The AZERO function disconnects the inputs internally and reads the internal offset voltage, which is subtracted from each preceding measurement. This function is used for both ohms and DC measurements. Just like the OCOMP function, this function also doubles the time taken for each reading. With both functions switched on, one measurement consists of two OCOMP readings and two AZERO readings. The "genuine" reading is the OCOMP reading with the source current on. The measurement sequence will be described further in chapter 3.2.1.

Because the source current is being periodically disabled with the OCOMP setting switched on, the thermistor only heats up a fraction of the time it would with the OCOMP setting switched off. With OCOMP on, the effective power dissipation can be approximated in terms of the power that would be dissipated, if the OCOMP setting were switched off, and the current had been constant, but lower. The measure for this effective dissipated power would be proportional to the ratio of the measured values for the resistance of the thermistor with the OCOMP both off and on. Figure 2 shows the difference in thermistor temperature with OCOMP on versus OCOMP off. The blue line is the actual temperature fluctuations; the green line represents the measured data for OCOMP on.

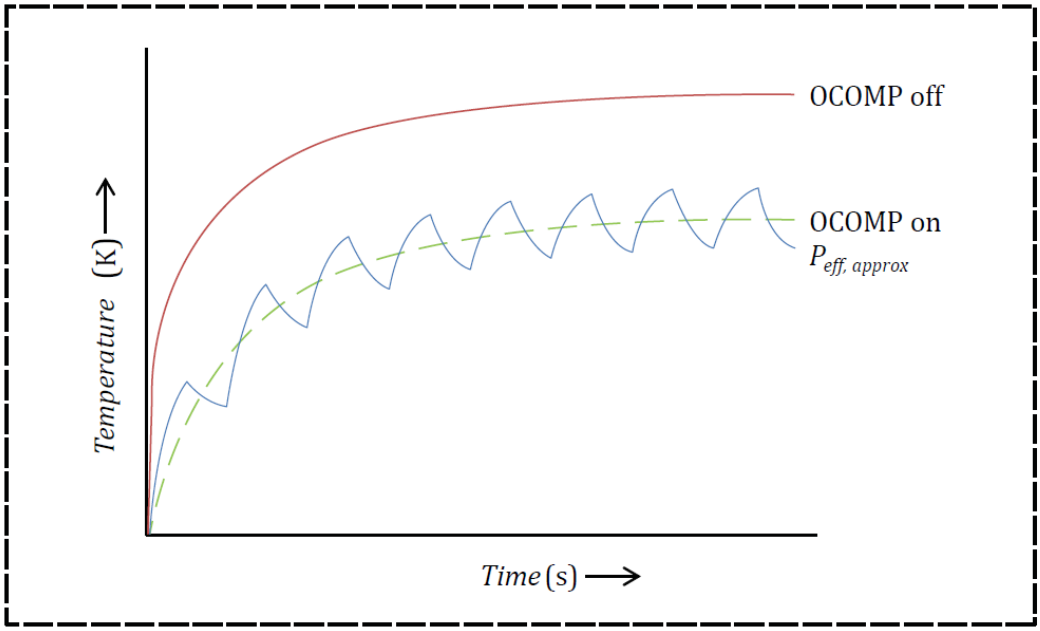

Figure 2 The thermistor temperature in time with OCOMP on- and off. For OCOMP on an approximation has been made of the net equivalent dissipated power

The equilibrium temperature with OCOMP on is based, mainly, on the integration time of the DMM, because that greatly influences the up- and down-time of the current. The expression for the effective dissipated power at equilibrium is given by:

$$P_{eff} = P_0 \cdot \frac{R_{OCOMP\ on}}{R_{OCOMP\ off}} \tag{20}$$

With:

P_{eff}	the effective dissipated power by the thermistor with OCOMP on	[W]
P_0	the total dissipated power by the thermistor with constantly applied current	[W]
$R_{OCOMP\ on}$	the thermistor resistance at equilibrium with OCOMP on	[Ω]
$R_{OCOMP\ off}$	the thermistor resistance at equilibrium with OCOMP off	[Ω]

The current up-time is, very nearly, equal to the current down-time. In the past, measurements have been done with NPLC = 10 and 20. (= Number of Power Line Cycles, a convenient measure for integration time based on the line frequency of the power supply (=50 Hz in Europe), 1 PLC corresponds to 2 ms. With integration times over 10 PLC, rather than continuing with integration times an integer value of 1 PLC, the DMM rounds the number up to the next n^{th} multiple of 10 and takes n readings of 10 PLC (DMM_manual, 2012, p. 325). These readings are averaged and outputted to the display/computer. There is a small delay at the end of the reading at 10 PLC. This delay is mainly used for outputting the value and sending it over the GPIB and/or to the DMM display. When measuring, using a larger integration time than 10 PLC, the said delay only appears at the n^{th} multiple of 10 PLC. That is the final integration period of the reading. Figure 3shows a schematic representation of the integration periods and delays for 10- and 20 PLC. As the ratio of current up-time and down-time alters with different NPLC settings, the effective dissipated power of the thermistor will change accordingly.

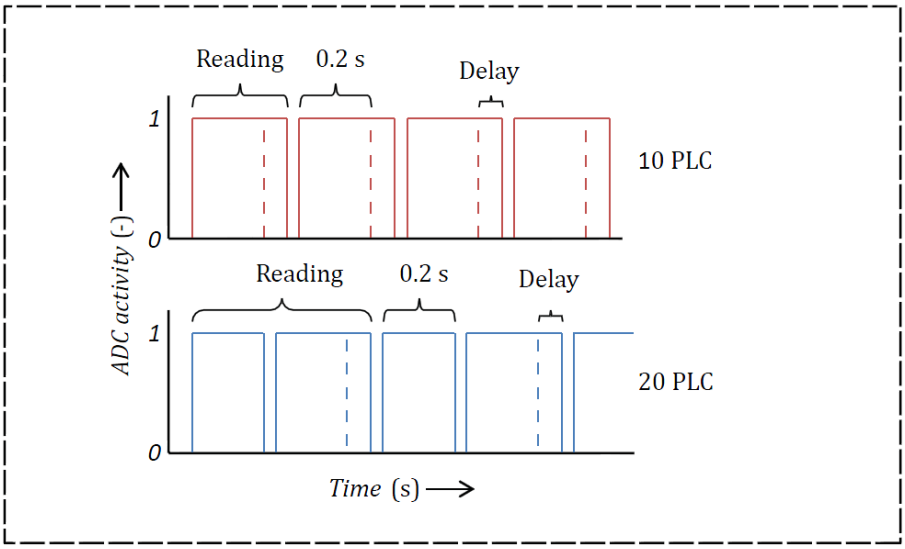

Figure 3 Schematic representations of the integration times with corresponding delays of 10 and 20 PLC

Equation (14) describes the heating of the thermistor with a constant current applied. The thermistor cools according to the same equation, except with the power input, P reduced to zero.

3 Measurement methods and materials

This chapter starts off by describing the used measurement set-up. The general measurement method will be discussed afterwards with a specific description for each individual aspect of the problem. These descriptions may contain additional theoretical background. This chapter is concluded with an introduction to the established uncertainty budget.

3.1 Measurement set-up

The measurement set-up used consists of the VSL water calorimeter with cool thermostat (Lauda RP845), three digital multimeters (Agilent/HP 3458A with option 002) and two thermistors (serial numbers: VSL05T067, VSL05T065).

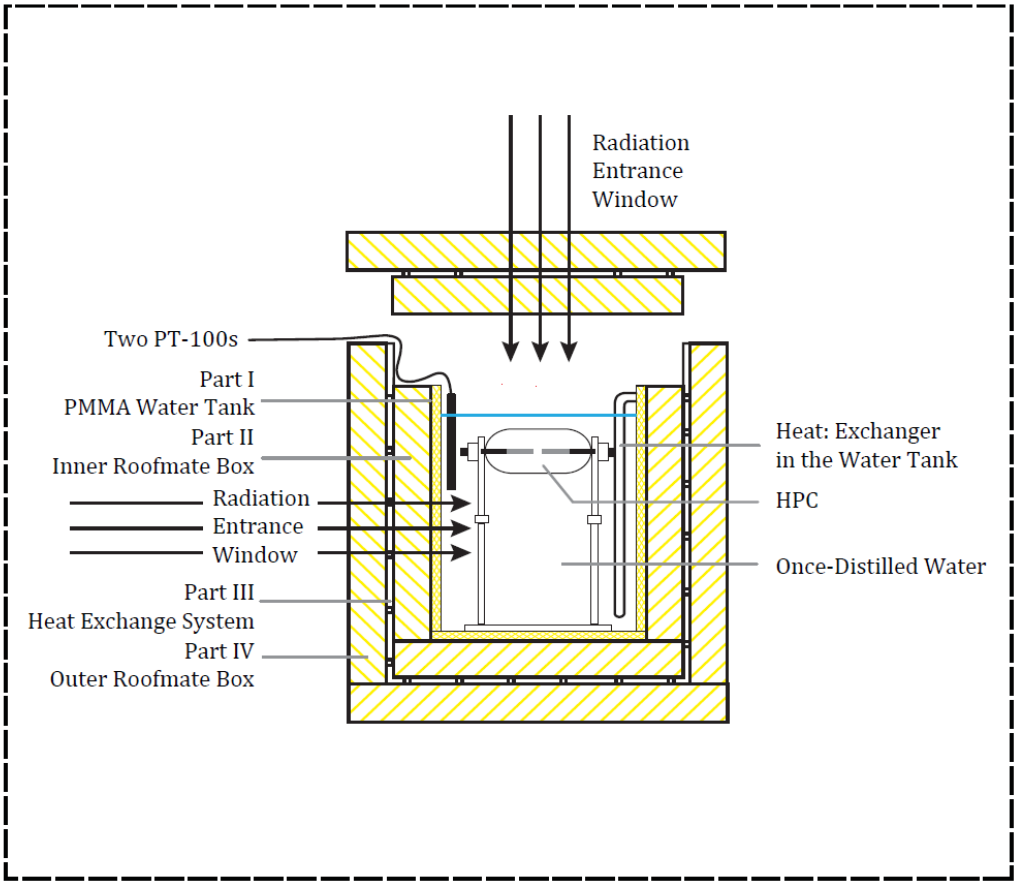

Figure 4 Cross-sectional view of the VSL water calorimeter

The VSL water calorimeter, WCM (Figure 4), consists of a water phantom, a 30×30×35 cm^3 made of Plexiglas (PMMA) filled until 5 cm below the edge with demineralized-water. There are two standards placed in the phantom to keep the HPC (high purity cell) in place. The thermistors are placed inside the HPC and are surrounded with ultra-pure water. The ultra-pure water in the HPC is closed from the rest of the water in the phantom. The phantom is surrounded by two layers of insulation material to thermally insulate the WCM from the surroundings as much as possible. Between the layers, copper plates with tubes mounted on them are placed. Through these tubes the cooling liquid of the Lauda cooler is circulated. The Lauda regulates the temperature of the copper plates using a PT-100 which is placed on the copper. A PT-100 is a moderately accurate thermistor to measure temperature.

3.2 Measuring methods

The resistance of the thermistor is being measured by a DMM using the 4-wire method with the OCOMP and the AZERO settings switched on. During one OCOMP measurement, the source current is disabled and the heating effect ceases. The on-and off switching of the source current results in a voltage square wave and makes the thermistor settle around a lower self-heat temperature than when the current is constantly switched on (=OCOMP OFF)(Figure 2). For an accurate determination of the self-heat of the thermistor, it is essential to know as accurate as possible how the resistance varies in time during the up-time (=source current on) and when, on this curve, the actual measurement is taken between the enabling and disabling of the source current. This can be achieved by sampling the voltage (sense) of the 4-wire resistance measurement by a second DMM. The resistance can only be measured when the source current is applied through the thermistor. The measured voltage follows the square wave of the current, except during the current up-time. The voltage and resistance will change slightly in time due to the self-heat effect. When enough samples are taken during one of these squares, the course of the resistance and thus the self-heat can be mapped. This is shown in Figure 5.

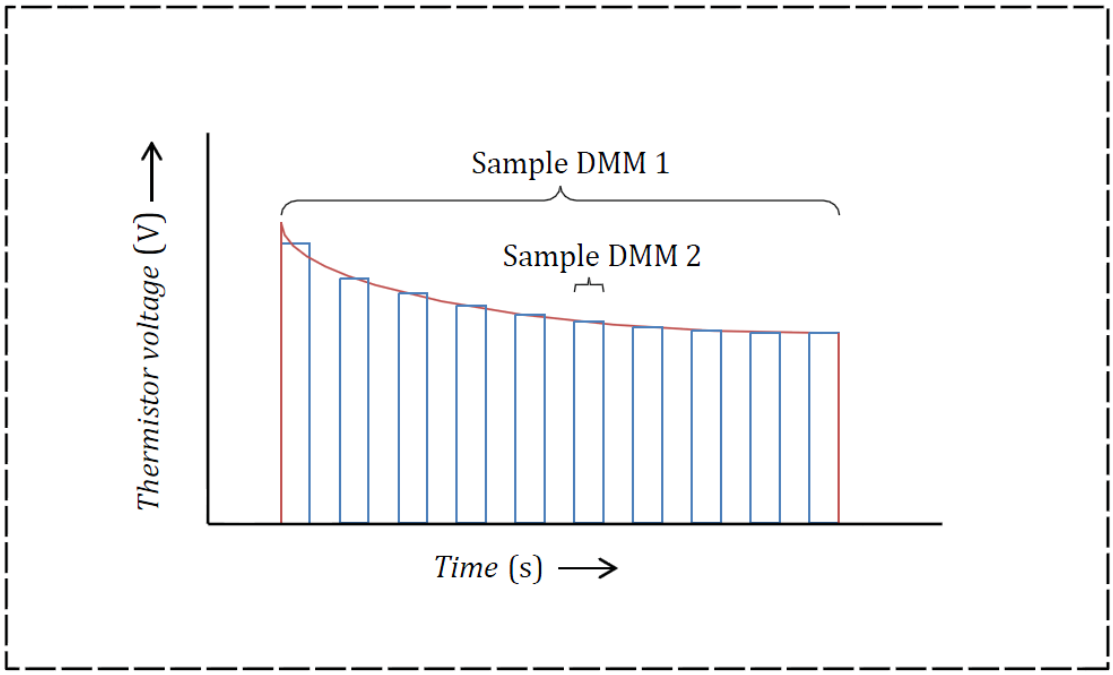

Figure 5 Schematic representation of the course of thermistor voltage during self-heating. The sample interval of the OHMF-DMM(1) and DCV-DMM(2) have been indicated (not to scale)

Notice that the thermistor voltage decreases during the time the source current is on. Because of the negative temperature coefficient (NTC) the voltage drops when the temperature rises.

This method reveals the change in resistance as source current heats up the thermistor. The DMM measuring the resistance integrates the signal over a period of time. This integration time does not fully correspond to the current up-time. There are delays like settling time and sending the data to the display and/or the GPIB bus. As the resistance keeps changing in time, it is important to know which readings are made when by the resistance-measuring DMM.

3.2.1 Measurement sequence and triggering

There are several ways to trigger the DMM. Triggering on an external device is usually faster than level- or automated triggers (DMM_manual, 2012, p. 298). The DMM has an option to send a trigger itself to an external device; the EXTOUT function. This is especially convenient when using two Agilent 3458A's. When specified, the aperture waveform event (APER event) outputs a waveform indicating when the analog to digital converter (ADC) is integrating the input signal (DMM_manual, 2012, p. 114). In addition to showing when a reading is being measured, the aperture waveform also shows any AZERO and auto range measurements being made. This waveform can be used to synchronize external switching equipment to the multimeter. With this synchronization, it is possible to determine on which part of the voltage curve the measurement has been done. The EXTOUT output can send a TTL-signal based on several events. A TTL-signal can be "high-going" or "low-going". The DMM can trigger on the ascending or descending slope of the TTL pulse. The specific event used for triggering is based on the activity of the ADC. When the ADC is active, e.g. integrating a signal, the DMM outputs a high signal, when it is not, it outputs a low signal. This waveform is called the "aperture waveform" and it can either be positive or negative based on the desired timing for triggering. Figure 6 shows some of the possible EXTOUT triggering events.

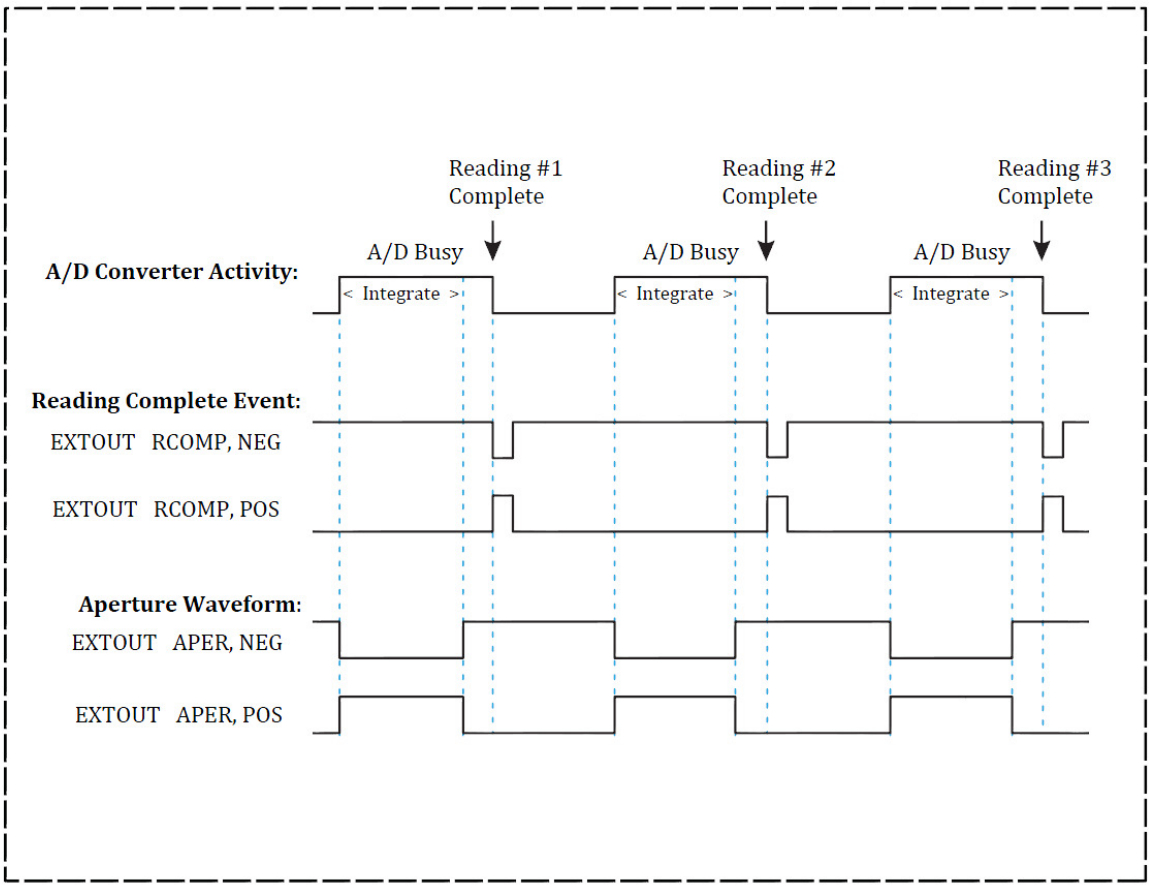

Figure 6 Several EXTOUT waveforms for possible triggering

During measurements, the negative version of the aperture waveform was used because the DMM always triggers on the descending flank of the TTL-signal. When the ADC starts integrating the slope will be negative and the DMM will receive a trigger almost exactly when the primary DMM is starting its measurement. The second DMM triggered by the EXTOUT, measuring the voltage of an OHMF measurement received four times the amount of triggers as the number of resistance-readings. This

indicates during one reading, the ADC is actually integrating the signal four times. Two of these integrations are OCOMP readings, which are compared with each other i.e. one reading with the source current on and one without source current. These individual OCOMP readings are each followed by an AZERO reading. Figure 7 shows a schematic representation of the voltage signal of an OHMF reading along with triggering corresponding to the negative aperture waveform.

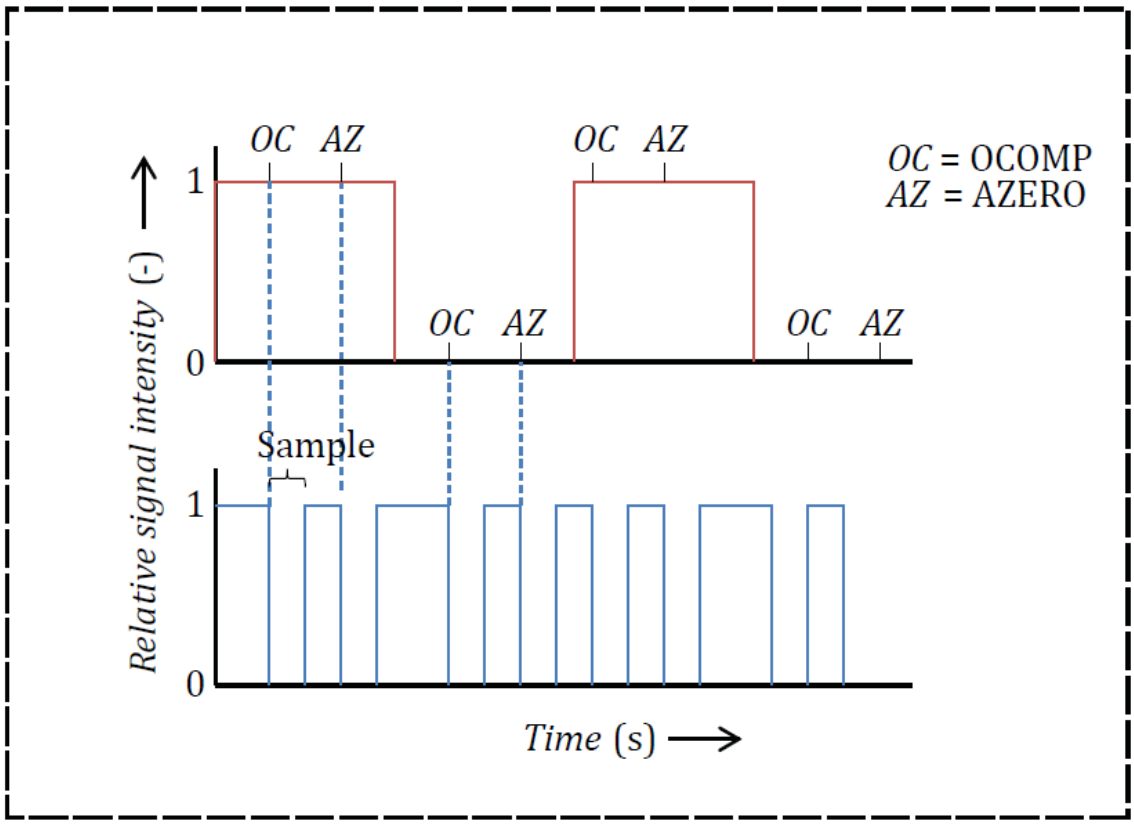

Figure 7 Schematic representation of an OHMF-reading with OCOMP and AZERO on, with its corresponding negative aperture waveform

The top graph is the resistor voltage during an OHMF-reading with OCOMP and AZERO enabled. The graph below shows the corresponding aperture waveform. Because the DMM triggers on a negative slope of the TTL-signal, the waveform needs to be low-going at the start of an integration. As seen, this can only occur by triggering using the negative aperture waveform.

The true resistance value is determined by calculating the difference between the OCOMP readings after they have been deducted by their internal offsets. Figure 8 contains a more detailed representation of the measuring sequence of an OHMF reading with the OCOMP and AZERO settings both on.

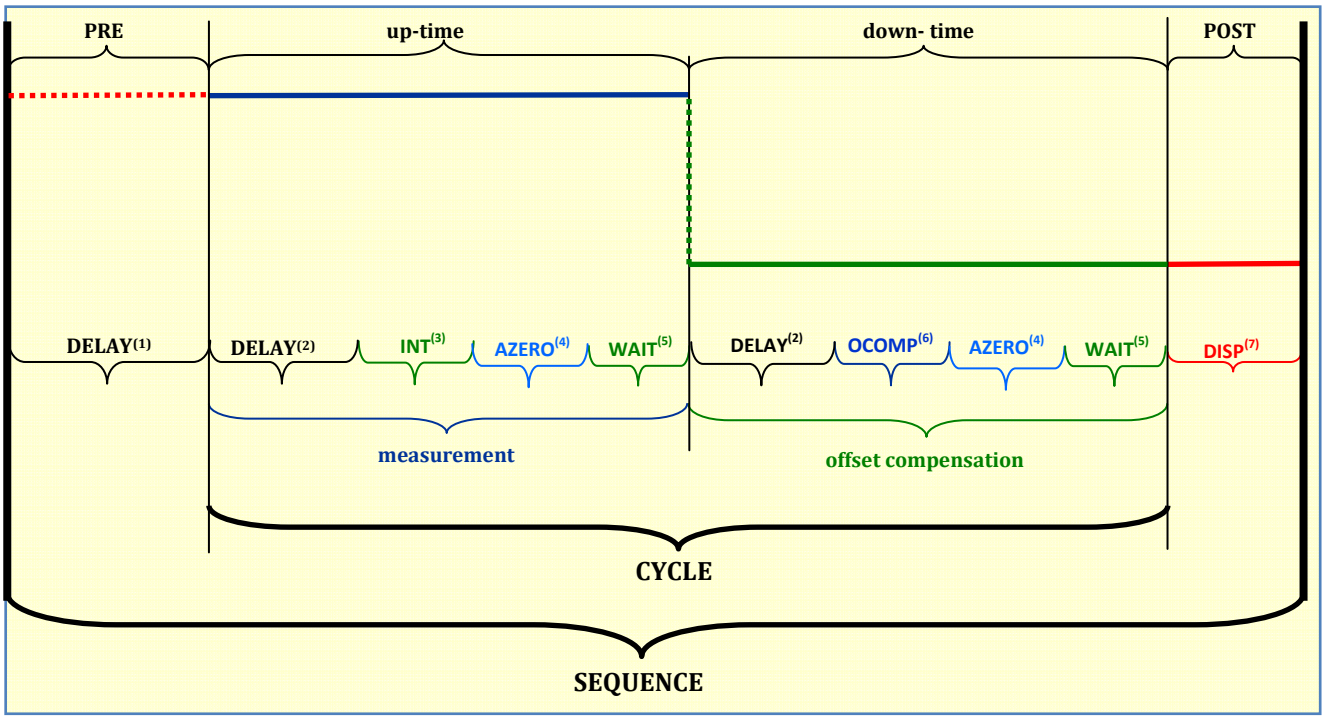

Figure 8 Schematic representation of the sequence of a resistance measurement with optional OCOMP and AZERO readings.

(1). Delay (OCOMP OFF); a variable delay between the trigger and the reading. This is kept minimal if no value is specified
(2). Delay (OCOMP ON); a variable delay. Replaces [1] if OCOMP is switched on
(3). INT; the main reading. With OCOMP ON, this reading is deducted by the second OCOMP reading (6)
(4). AZERO (AZERO ON); the AZERO reading corrects for internal offsets after every integration. This is done twice every reading with OCOMP ON and AZERO ON. Only once per measurement with AZERO OFF/ONCE
(5). WAIT; a delay to correct for the AZERO and OCOMP.
(6). OCOMP; the OCOMP reading done with OCOMP ON to correct for external voltage offsets
(7). DISP; a 20 ms delay in which de DMM sends data to display. Can be avoided by disabling the display

Each measurement consists of the “sequence” part, where the “cycle” part is repeated until the number of readings set has been satisfied. The duration of the delays are variable, but restricted by a minimum, as there might be a desired delay between the trigger- and sample events. The duration of all integrations done by the ADC are set with the NPLC or APER-values.

3.2.2 Custom measurement program

Some of the desired measurement cannot be done by the program used to read out the data from regular water calorimeter measurements. That program can only retrieve single samples at a time which required a lot of time to transfer. When the sample frequency is increased, it will reach a point at which the DMM gets readings at a faster pace than it can send. To be able to monitor the resistance of the thermistor a new program was written to be able to retrieve data fast enough to be able to map the course of the thermistor resistance. Shortly hereafter, the program was updated to command and retrieve data from two, and later three DMMs.

The DMMs are given a number of settings in the initialization sequence. This sequence presets the DMMs to measure with specific settings i.e. integration time, sampling frequency and Delay. The interface of the program can be seen in Figure 9

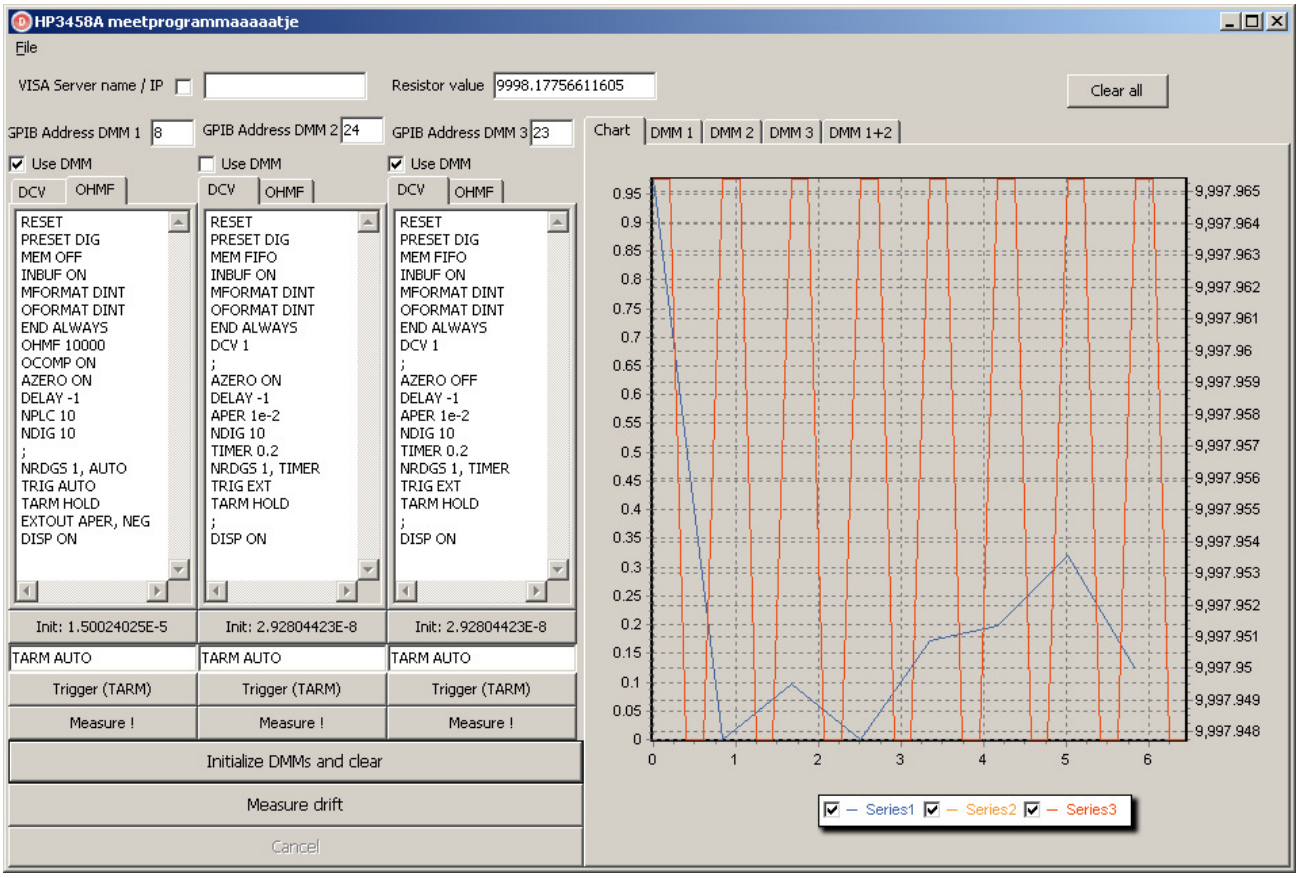

Figure 9 A screenshot of the interface of the custom made measurement program

On the left, three panes are visible. These panes contain the initialization commands for the three DMMs. these can be initialized separately or all at once. The text boxes below the individual initialization buttons contain the trigger arm command. This is done separately because the DMMs will start measuring once their trigger is armed and the trigger event is satisfied. This also gives more flexibility in the order of sending the trigger arm command. The "Measure drift" button sends the trigger arm command to all DMMs in a preset order. In this case, the OHMF-DMM receives the trigger arm command lastly. The Measure drift button also reads out the read-memory of the DMMs and plots the data as shown in the right part of Figure 9. The chart is shown on the first of five tab sheets. The second, third and fourth show display the measurement data along with a time stamp of the DMM corresponding to the initialization panes, left being the first. The final tab sheet is used to display the result of a mathematical operation done with the data of DMMs.

The DMMs are set to make a number of readings when the trigger- and arm events are satisfied. The program was set-up in a way that the DMMs would receive a single trigger arm command. The made readings will be sent to the program which will process them. The program will then send another single trigger arm. The DMMs will make readings and send them to the program again. This process continues in a loop until a "cancel" button is pressed. At each of these loop iterations a timestamp is given to accompany the readings. This way the readings can be plotted with the correct timeframe. To make sure all DMMs make readings at the same time, the two DCV-DMMs are triggered externally to the aperture

waveform of the OHMF-DMM. The latter is triggered last, so the two DCV-DMMs are 'waiting' for the OHMF-DMM.

Settings of the DMMs can be altered to change, including, but not limited to, their measurement function, integration time or sampling frequency. Several settings appeared to have a significant influence of the measurement results and need be set in a certain way or the program will not function properly.

DISP ON: This switches on the display. Switching this off will result in five sample points during the first OHMF-reading. After this it will revert to four and the timestamps will be out of sync. The origin of this problem is unknown.

MEM FIFO: The reading memory is switched to FIFO, First-In-First-Out. The measurements are outputted in the order they are obtained. Other options are LIFO, Last-In-First-Out. This function fills the reading memory until the controller requests data. When data is requested, it is outputted in reversed order. This will make drift measurements hard to interpret when the number of times the data is requested is greater than two. With MEM OFF, the DMM outputs the data samples obtained after the last measurement trigger. With OCOMP on, this is a zero-current reading and contains no useable information

OFORMAT DINT: This command sets the output format to DINT, double integer. The measurement data is compressed to integers using a scaling factor, which alters with variations with measurement function, -range, -ADC configuration math operations. Using integers rather than ASCII characters, reduces the data needed by a factor four.

END ALWAYS: When using OFORMAT ASCII, the ASCII characters themselves contain the line-feed and carriage-return bits. The double integers sent with OFORMAT DINT do not contain these bits. END ALWAYS ensures individual samples are not sent as one number, but retain their format.

TIMER: The TIMER command sets the time between the starts of two readings, which reciprocal is known as the sampling frequency. This time includes the time needed for the integration by the ADC. When the time needed for the integration of the sample exceeds the time set with the TIMER command, the DMM skips the received trigger and will start measuring with the first satisfaction of the trigger arm event after the previous reading has been finished. This time, unlike most number related commands with the DMM, does not accept the "E-notation" for powers of ten. This has to be written as a decimal number.

APER: Sets the integration time of the ADC in seconds. The recommended maximum of this value is one tenth of the value set for TIMER with OCOMP and AZERO both on.

NRDGS, EVENT: Sets the number of readings that will be made once the trigger is armed and the trigger event is satisfied. Possible events include, but are not limited to: "EXT", the EXT TRIG input, "AUTO", as soon as the controller requests data or "TIMER", with a specified time interval between the start of two readings.

TARM: During initialization the trigger is unarmed, or on "hold". The DMMs can be initialized and will wait until both the trigger arm event, as the trigger events are satisfied. Clicking the "Measure drift" button sends the trigger arm command and the DMM starts measuring as soon as the trigger arm- and the trigger events are satisfied. Giving the OHMF-DMM a single trigger arm was considered. When each DMM is read out, the OHMF-DMM would receive another single trigger. This makes the speed of the program direct how fast the measurements are done. It was believed the measurement program would not be fast enough to process all the data and slowing the measurement sequence down to the speed of the program could be beneficial. However, the system with the single triggers somehow caused the DCV-DMMs to not do any readings.

The custom measurement program is described further in Appendix IV Writing a custom measurement program.

3.3 Determining the current stability

Instability in source current is compensated for in the OHMF-mode. The voltage ratio of two resistors is determined (chapter 2.4.2). Current fluctuations occur at both resistors and are canceled out in the calculation of the ratio. Fluctuations in the self-heat due to the instability of the current source however, still persist. For any current fluctuation, the self-heat will fluctuate quadratically, see equation (3).

The Agilent 3458A digital multimeter has a built in setting for measuring direct current; the "DCI"-mode. However, this DCI-mode, with a long-term stability of about 25 μA/A (hereafter denoted as "ppm") is not as accurate as the DCV-mode, which has a long-term stability of 10 ppm (DMM_manual, 2012, pp. 284-286). Therefore a resistor with predetermined resistance and corresponding stability is used instead of a thermistor. While one DMM is measuring the resistance using the OHMF-mode, another DMM will monitor the voltage over the resistor. The measurement circuit is shown in Figure 10.

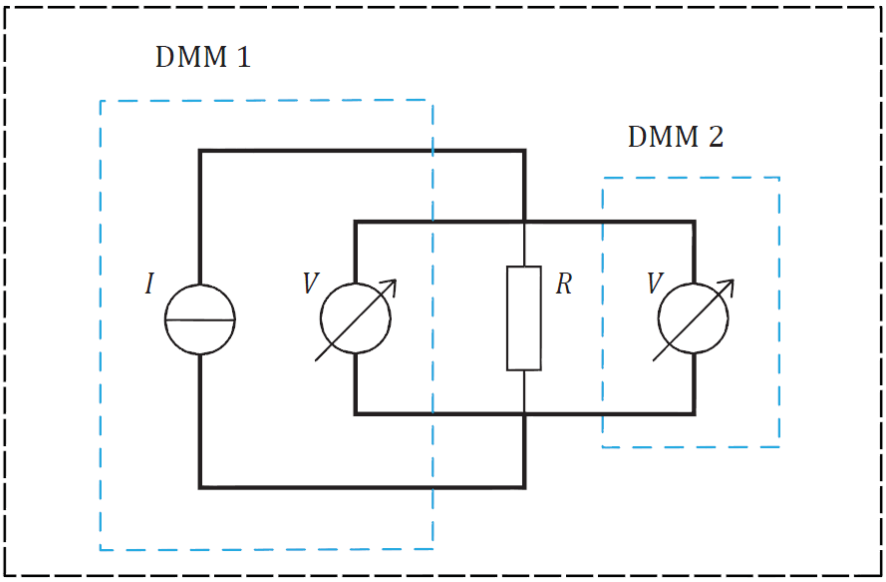

Figure 10 The electric circuit diagram of the current stability measurement

The fluctuations in voltage will correspond to a fluctuation in source current provided by the first DMM. The current will be calculated from the known resistance and the measured voltage with Ohm's law

$$I = \frac{V}{R} \tag{21}$$

With:

V the measured voltage over the resistor [V]

The measurements are done with AZERO and OCOMP both on. The current is measured in the 100μA range of the DMM. The resistor used in this measurement is the 10kΩ resistor of the Ionizing radiation department, named "R1". This resistor is measured in the 10kΩ range using the four-wire method and its voltage is measured in the 1V range.

3.3.1 Measurement method acceptance test

A different measurement method has to be verified to test if the measurement results are a realistic representation of the truth. A statistical test based on the measurement data of the tested method and a reference method will determine whether the different method is acceptable within a certain tolerance. The test checks if a measured sample, P_2, could be an element of a reference sample, P_1, with a certain level of confidence. The standard uncertainties of these samples are included in the calculation, which is done according to (Chatfield, 1996).

$$x = \frac{|P_1 - P_2|}{\sqrt{u_{P_1}{}^2 + u_{P_2}{}^2}} \tag{22}$$

With:

x	the EN-test result	[-]
P_1	the reference sample	[-]
P_2	the sample under test	[-]
u_{P_1}	the standard uncertainty in P_1	[-]
u_{P_2}	the standard uncertainty in P_2	[-]

For the tested sample to be accepted, the value calculated in x will have to be equal or smaller than 2. This corresponds to the minimum probability of 5 % that the tested sample will be rejected. When the sample is accepted it indicates that P_1 and P_2 are sufficiently coherent. In this test, the assumption is made that the uncertainties of both samples are normally distributed.

3.4 Effective power dissipation

As mentioned in chapter 2.4.3, the value of the OCOMP setting determines whether a current is constantly applied over the thermistor or disabled periodically. Even a change in integration time influences the power dissipation of the thermistor and thus, the self-heat. The course of the resistance of the thermistor can be mapped with OCOMP enabled and disabled. When a function can be found to fit these courses, the self-heat can be predicted more accurately based on the up- and down-time of the current. That concerns different NPLC, which have different numbers of delays which affect the ratio of time the current is enabled or disabled. Even when the integration time exceeds 10 PLC and it is rounded up to the next multiple of 10, the time needed for several delays will vary with respect to the integration time (see Figure 3).

The described differential equation (19) will be verified and fitted to test if it can be used to predict the heating of the thermistor during the complete heat-up phase, not just at equilibrium(20).

3.5 Resistance verification

A stabile resistor, with a well-known resistance is needed to measure the current. Three resistors have been measured to accurately determine their resistance. Resistors used as a shunt have to be tested for accuracy and stability. A shunt is a resistor used in current measurements. Typically shunts have a very low resistance and high stability to be able to measure large currents in a circuit. Technically, the used resistor is less suitable for large currents, but since current is being measured and for clarity, the term “shunt” is used for the resistor used for current measurements.

Using two DMMs to measure the thermistor current and the voltage applied could give resistance measurements with lower uncertainties than with just the OHMF-mode. To validate this, a reference resistor will be measured by one DMM using the OHMF-mode. The other two DMMs will measure the current and the voltage applied independently. The current will be measured using a shunt and measuring the voltage applied by the current. The correct execution of this method requires an insight in how exactly the 4-wire resistance measurement is done by the Agilent 3458A. Figure 11 shows how the unknown resistor is compared with the internal reference. When the shunt is placed between R_{DUT} (Device Under Test) and R_{REF} (in gray), The voltage over the shunt is influenced by the shunt being placed parallel with the entrance impedance of the voltmeter. This results in a measurement error of about 100 ppm.

The DMM drives a current through two wires, the "input high" and "input low". The input low returns through an internal resistor in the DMM. This is the reference resistor for the DMM. The DMM measures the voltage over this R_{ref}. With the "sense high" and the "sense low", the DMM measures the voltage over the unknown resistor. The voltage ratio corresponds to the ratio of the resistors, thus automatically compensating for any instability in the current.

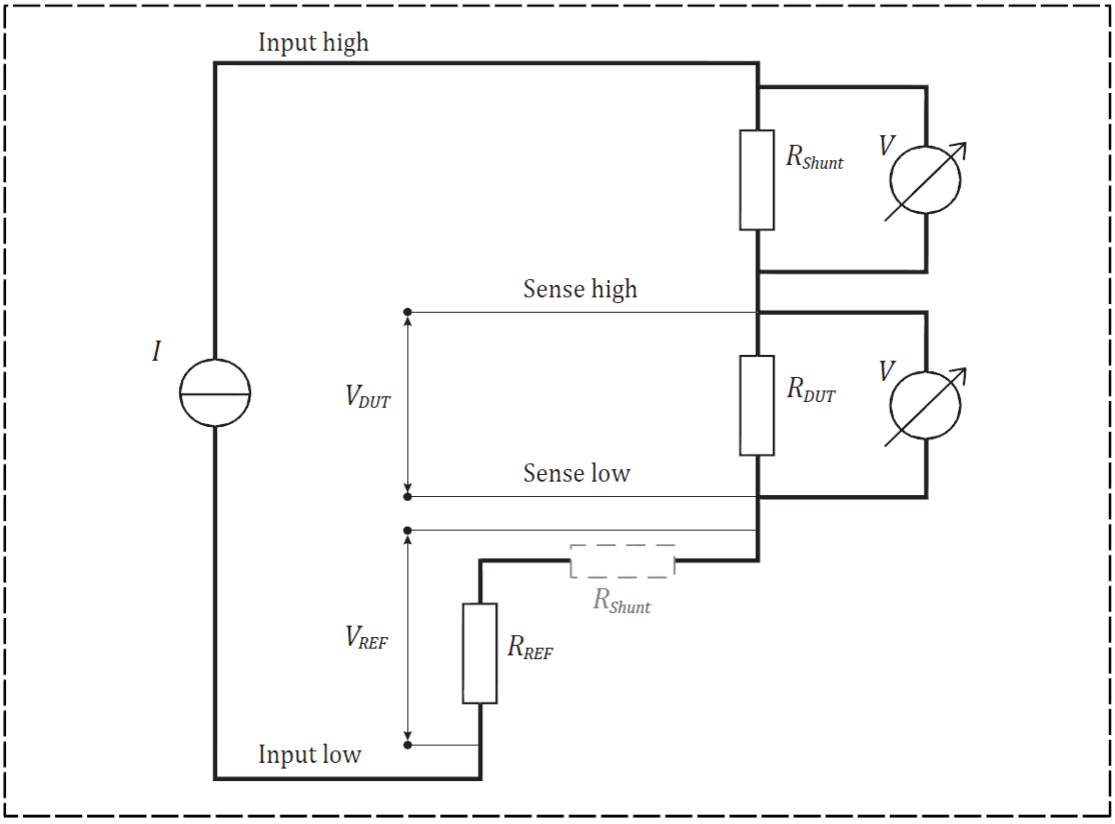

Figure 11 The measurement set up for resistance verification with three DMMs. With the incorrect location of the shunt marked in grey

The resistance can be calculated with the two DMMs connected properly using equation(21)

$$R_{DUT} = \frac{V_{DUT}}{I_{DUT}} = \frac{V_{DUT}}{\frac{V_{shunt}}{R_{shunt}}} = \frac{V_{DUT} \cdot R_{shunt}}{V_{shunt}} \tag{23}$$

With:

R_{DUT}	the calculated resistance	[Ω]
V_{DUT}	the voltage over the resistor	[V]
I_{DUT}	the current through the resistor	[A]
V_{shunt}	the voltage over the shunt	[V]
R_{shunt}	the resistance value of the shunt	[Ω]

However, there will still be a difference with the four-wire measurement. This DMM subtracts offsets with the OCOMP measurement. Because the other two DMMs are also sampling the offset voltage when the source current is disabled, this offset can be corrected for manually. With the known timing of the integration of the four-wire measuring DMM, samples can be taken at the correct time interval and be adjusted with the corresponding OCOMP values. The found resistance values will be compared using the EN-test.

3.6 Uncertainty budget

This chapter describes the uncertainty budget is established is and will start with the basic concept of uncertainty analysis. The general contributions to the uncertainty will be discussed first. The complete uncertainty budget with uncertainties of the measurements done is included in chapter 4.5.

The uncertainty of a result is no less important than the value of the result itself. One might even say the result is meaningless without associated uncertainty. In metrology, uncertainty has high priority. In production lines the wish is to stay within the margins of uncertainty. In metrology every reduction in the uncertainty is being fought for.

There are two fundamentally different concepts when it comes to uncertainty analysis. “Uncertainty” and “error”. These might appear similar, but they cover completely different parts of the eventual uncertainty of a found value. Uncertainty is a margin in which a measurement, if the experiment was repeated exactly, would fall in, with a certain level of confidence (usually about 95 %). The error of a measurement is the constant deviation of the correct value. When equipment is calibrated and a perfect 1 V signal is presented. The DMM could indicate 8 V. This would appear as a faulty device and it should be replaced. However, if the uncertainty in this measurement was ±1 pV, then it might be wise to use that DMM as the primary DMM for accuracy measurements. The uncertainty in this example is the margin of ±1 pV and the error would be +7 V. Errors are structural measurement defects and can be compensated for. Calibration certificates show the presented value, the measured value and the uncertainty in that measured value.

The uncertainty in a measurement consists of two ‘types’. “Type A” and “Type B”. Type A uncertainty is established by statistical means. This uncertainty is determined by repetitive measurements, e.g. by the spread of measured values around an average. When the spread is small, the estimated value of a certain physical quantity has a lower uncertainty than when the spread is wider. Also the amount of measurements done plays a role in the uncertainty. When five measurement values nearly overlap each other, the uncertainty can still be higher as where a larger spread is obtained from thousands of measurements. This relation is described by

$$u_{Type\ A} = \frac{s}{\sqrt{n}} \tag{24}$$

With:

$u_{Type\ A}$	the Type A uncertainty of a sample	[-]
s	the standard deviation of the sample	[-]
n	the number of samples taken	[-]

Type B uncertainties are the uncertainty estimates from by other means. This could be information from device specifications, calibrations, past experience and common sense. Where the Type A uncertainty is considered a "normal" or "Gaussian" distribution. The measured data is more likely to be closer to the mean than further away, the Type B uncertainty can have other distributions, like a rectangular distribution. This distribution means that a value is evenly likely to be near the upper- or lower limit of a taken interval as in the middle. For example: snowflakes on a thin wire. The flakes are evenly likely to fall on each part of the wire. The standard uncertainties of different distributions are calculated differently. The standard uncertainty of a rectangular or "uniform" distribution is calculated as follows:

$$u_{rect} = \frac{a}{\sqrt{3}} \tag{25}$$

With:

u_{rect}	the standard uncertainty of a rectangular uniform distribution	[-]
a	the half-width between the upper and lower limits	[-]

To determine an uncertainty when it depends on multiple factors, these uncertainties have to be added. The uncertainties have to be expressed in the same units and the same level of confidence. Relative uncertainties are useful to express the uncertainties in the same units, dimensionless. The level of confidence depends on the distribution. As shown above, the rectangular distribution and the standard uncertainty of the mean are expressed with the same level of confidence.

The relative uncertainties are combined using quadratic addition. Combined with the relative uncertainties mentioned above, the expression for total the total relative uncertainty looks like this:

$$\frac{u(B)}{B} = \sqrt{\sum_{i=1}^{N}\left(\frac{u(X)}{X}\right)^2} \tag{26}$$

With:

$u(B)$	the uncertainty in the arbitrary physical quantity B	[-]
B	the arbitrary physical quantity B	[-]
$u(X)$	the uncertainty in the arbitrary physical quantity X	[-]
X	the arbitrary physical quantity X	[-]

The individual uncertainties can depend on multiple variables. These uncertainties can be found by partial differentiation. In essence, this gives the sensitivity of a function to a specific variable. A higher sensitivity to a variable means that the uncertainty in this variable will have a greater impact on the uncertainty of the determined physical quantity. Consider the example below where *X* has dependencies of *V* and *W*. The relative uncertainty of *X* would then be given by:

$$\left(\frac{u(H)}{H}\right)^2 = \left(\frac{\partial H}{\partial F}\cdot\Delta F\right)^2 + \left(\frac{\partial H}{\partial G}\cdot\Delta G\right)^2 \tag{27}$$

With:

$u(H)$	the uncertainty in the arbitrary physical quantity H dependent of F and G	[-]
H	the arbitrary physical quantity H dependent of F and G	[-]
F	an arbitrary physical quantity	[-]
G	an arbitrary physical quantity	[-]

Combining equations(24), (26) and (27) result in finding the combined standard uncertainty. This level of confidence of this combined standard uncertainty is based on that of a normal distribution, which means that ≈68 % of the values of the measurements done, are covered by the specified uncertainty. The 68 % is based on the standard deviation of a normal distribution. When a larger coverage factor is desired, the combined standard uncertainty is multiplied by a factor, *k*, which corresponds to a number of standard deviations of coverage.

$$U = ku_c \tag{28}$$

With:

U	the expanded uncertainty	[-]
k	the coverage factor	[-]
u_c	the combined standard uncertainty	[-]

Some coverage factors for the normal distributions are:

k = 1 for a confidence level of approximately 68 %
k = 2 for a confidence level of approximately 95 %
k = 3 for a confidence level of approximately 99.7 %

Note that these coverage factors only apply for normal distributions. Also note that non-integer values might also be used as coverage factors depending on the desired level of confidence. For example, a level of confidence of 99 % requires a coverage factor of 2.58. To calculate these values, the Gauss equation for the normal distribution has to be solved. This however, is not necessary in metrology, where usually integer values for *k* are used, which does not exceed 3.

3.6.1 General contributions to the uncertainty

Changes in a laboratory environment, like temperature and humidity, play a role in the accuracy of measurements done. These factors influence all measurements to some extent. This paragraph discusses the contributions to the uncertainty which occur in (nearly) all of the measurements.

All measurements were done using one or more Agilent 3458A, option 002 digital multimeters. The option 002 indicates a high stability option of the model Agilent 3458A DMM. The used measurement functions are the DCV (direct voltage), DCI (direct current) and OHMF (four-wire ohms). The DMM has different accuracy, temperature dependency, and noise and gain errors for each of these modes. Table 1 contains a general overview of these uncertainties.

Table 1 A general overview of uncertainties with different measurement functions as is presented in the specifications of the DMM (DMM_manual, 2012, p. 284)

Uncertainty origin	DCV (1 V range)	OHMF (10 kΩ-100 kΩ range)	DCI (100 µA range)
Accuracy (ppm reading + ppm range)	12 + 1	25 + 8	15 + 1
Temperature (ppm reading + ppm range)/K	0.15 + 0.1	2 + 1	1 + 0.1
Noise (ppm range)	2	30	0.2
Gain (ppm reading)	5	4	2
Linearity (ppm reading + ppm range)	0.3 + 0.1	-	-
Combined uncertainty (ppm of range + ppm of reading)	**13 + 2.3**	**24 + 31**	**15 + 1**

The before mentioned uncertainty due to the humidity has not been taken up in the table above. The influence on measurements of the humidity can be significant, but this effect is very slow. The humidity characteristics of the Agilent/HP 3458A can, and is measured in VSL. Humidity changes slowly and affects the electronics in the DMM even slower. Therefore, these measurements usually take weeks to even measure the characteristic of the humidity of a specific DMM. This indicates that these effects are negligible in an environment where the relative humidity is actively kept controlled to 45 %.

The previously mentioned errors in the DMM are called *y*-axis uncertainties, because these uncertainties affect the amplitude of the measurement. There are also *x*-axis uncertainties, which are time based errors caused by imperfections of the DMMs internal clock or external time-based events. These potential errors, or uncertainties, tend to be very small relative to the used integration times. (DMM_manual, 2012, pp. 297, 361). This can include errors based on jitter in the aperture and trigger, aperture width and trigger latency. Almost all of these errors are smaller than 100 picoseconds. The trigger latency with external triggering can be up to 175 ns (DMM_manual, 2012, p. 295), which still is significantly smaller than the used aperture times of >1 ms. The reading error in AC sub-sampling measurements is found to be at most 1 ppm for frequencies lower than 100 kHz (Swerlein, 1989). In this case direct sampling has been used and there is reason to believe that with direct sampling of DCV signals, this error has equal magnitude.

3.6.2 Calibration uncertainties

A lot of equipment has to be calibrated to validate the function the equipment is designed for can be executed with a certain level of tolerance. A calibration is a mapping of a device's error and uncertainty. Table 1 shows the relevant data from a calibration certificate of a DMM. All used data from certificates may be found in Appendix V Calibration certificates. The accuracy of the measurements provided by the manual can be substituted by the uncertainty in the certificate, once the correction for the error has been made. There still has to be corrected for the drift.

Table 2 Fragment of the VSL calibration certificate of the Agilent 3458A opt 002. Serial number: US28029799; certificate number: 3351760

Range (V)	Presented value (V)	Measured value (V)	Uncertainty in measured value (μV/V)
1	0.970 000 0	0.970 005 6	2
1	0.980 000 0	0.980 005 7	2
1	0.990 000 0	0.990 005 7	2
Range (kΩ)	Presented value (kΩ)	Measured value (kΩ)	Uncertainty in measured value (μΩ/Ω)
10	1.900 00	1.899 99	100
10	10.000 00	9.999 93	25
100	19.000 0	19.000 0	30
100	100.000 0	99.999 6	10

The provided uncertainties and errors substitute the accuracy values provided by the specification sheets of the manual (appendix A, Agilent 3458A manual, page 284). These accuracies then give an approximation of the drift of the DMMs.

4 Results

This chapter discusses the results found doing the measurements with the corresponding measurement methods discussed in chapter 3. This chapter will conclude with the complete uncertainty budget of the measurements.

4.1 Sampling of the resistor voltage

Initially, a fast sampling of the voltage (=sense) was performed over one thermistor, present in the water calorimeter. During this sampling a periodic interference signal was discovered. Using the sampling frequency of the DMM, the frequency of the interference signal was approximated to be about 50 Hz. To rule out any possibilities of internal interference, a number of variables were altered. One of the variations was applied to the sampling frequency. It was assumed that if the interference was internal, the frequency would follow the alteration of the variables in some extent. However the interference continued to be present and its frequency was the same. This strongly suggested interference from the power supply. A number of tests were done to rule out interference of other devices. It was discovered that the Lauda cooler was involved in the interference as can be seen in Figure 12. The blue line represents the zero-measurement, or the baseline measurement. The interference signal was discovered in this dataset. This graph was then used to see if the adjustments improve the signal-to-noise ratio. The red line shows the data when the Lauda cooler was switched off and its PT-100 disconnected. However, in the actual WCM measurements, the Lauda had to stay on to cool the water phantom. The green data was obtained by setting the DMM guards to "open" and connecting all the grounds of the DMMs and the Lauda as well as the copper casing. The copper casing seemed not to be only conducting the temperature of the coolant equally, but also was the cause of electrical leakage from the power mains, which interfered with the thermistors. This increased the signal-to-noise ratio by a factor 34.

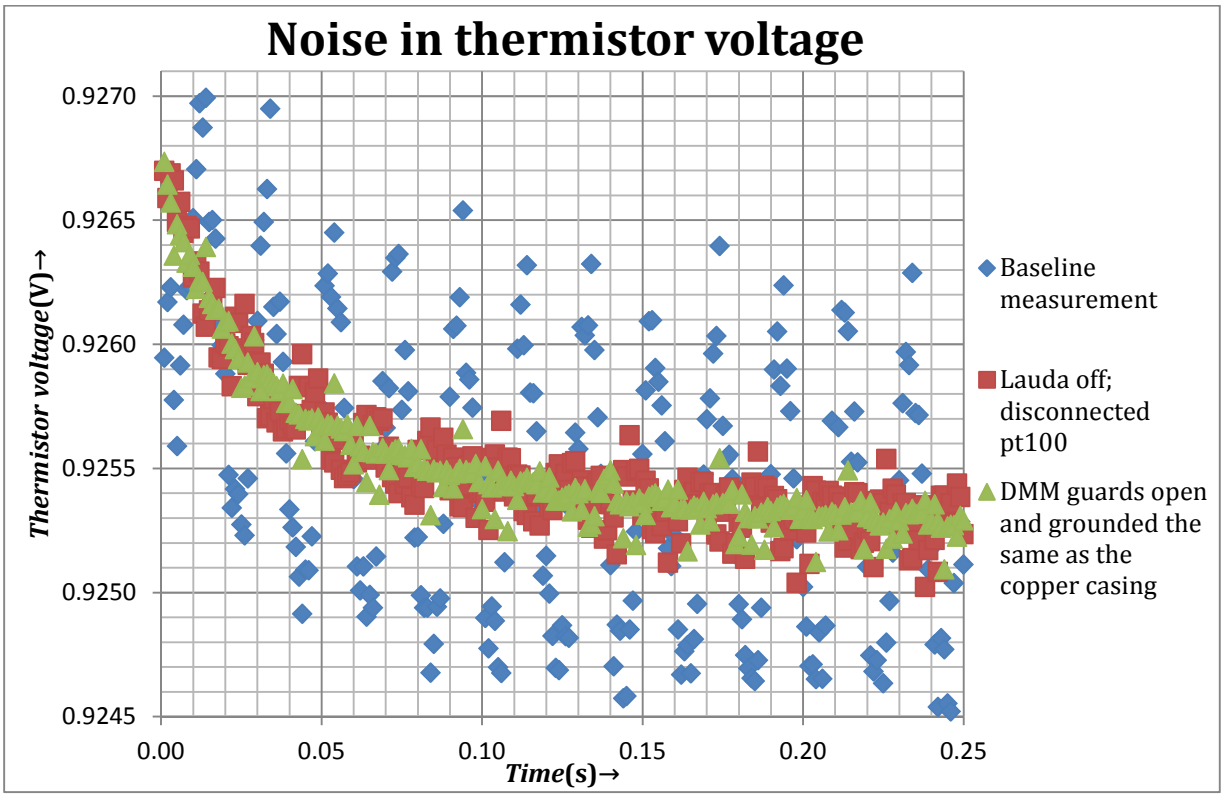

Figure 12 Plot of the sampled data of the thermistor self-heat during a fragment of one OHMF-reading

4.2 Current stability

There are several ways to determine the electrical current driven through a resistor by a DMM, and thus, to determine the stability of that current. The OHMF-mode uses voltage ratios to compensate for fluctuations in the current, but the thermistors self-heat might still be affected significantly by any fluctuations of the current. Below are two examples of how to measure the current supplied by a resistance-measuring DMM:

1. Shunt-method: Using a stable shunt resistor and measure its resistance with a DMM in the OHMF-mode. Sample DCV (sense) over the resistor and divide this by the measured resistance to retrieve the applied current.
2. DCI-method: Connecting a second DMM in series and using the DCI mode. However, this method is relatively uncertain, but reliable; i.e. the measurement itself it not likely to go wrong with the developed measurement program. This method is best used to verify other methods.

The current measurement with the DCI mode resulted in a current value of 97.5334 μA ± $3.7 \cdot 10^{-3}$ μA. The DCV-mode resulted in with $k = 2$. 97.5308 μA ± $3.8 \cdot 10^{-3}$ μA, with $k = 2$, with standard deviations of $35 \cdot$ μA/A for the DCI-mode and 11 μA/A for the DCV-mode. Which indicates the current to fluctuate within 1 nA in 68 % of the time when measuring in the 10 kΩ-range.

The DCV-method has a lower uncertainty than the DCI mode. This mode will be used in the measurement for the resistance verification, also because fluctuations in source current are a point of interest as this information is unavailable in OHMF-measurement.

As mentioned before, the long-term current stability of the DMMs is a significant contributor to the uncertainty budget. The used DMMs are known for their stability and usually perform well within specifications. One DMM was calibrated for DCI, which had not been done since it was acquired, over ten years, and it showed that its drift is well within one-year specifications. The usage of the two-year drift specifications is pessimistic, but makes that the uncertainty budget can be used at any point within the two-year calibration cycle of these DMMs. The fact that these DMMs perform so often within their specifications indicates that the uncertainties in the drift of the DCV- and OHMF-modes are too large. The short term drift of these modes is only a fraction of their long-term drift.

4.3 Resistance verification

The resistance of two parallel, 20 kΩ resistors was measured using two methods. One method uses the OHMF-mode of the DMM. The other measures the voltage and the current of the resistors separately. From which, the resistance value may be calculated. To measure the current, a shunt was placed in series and the voltage over it applied by the source current was measured. With the known resistance of this shunt, the current may be calculated.

Figure 14 contains a fragment of the measurement data with both methods. The blue graph shows the OHMF-method. The red graph shows the calculated resistance using two DCV-DMMs and the resistance value of the shunt. Both graphs contain their respective error bars.

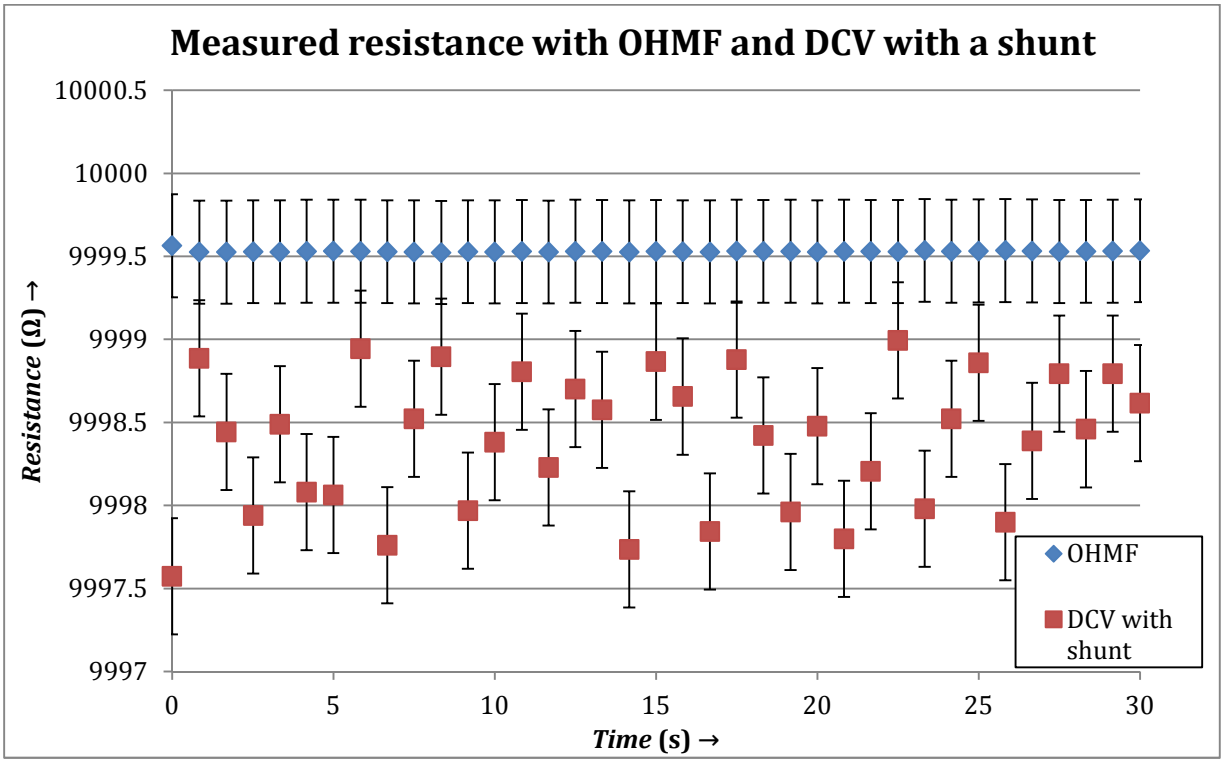

Figure 13 Measured resistance of two parallel connected resistors using the OHMF-method and the DCV-method with a shunt

The OHMF-method shows a very stable line, which is also reflected by a low standard deviation of a mere 7 mΩ. The other method shows a large standard deviation 400 mΩ and an offset of about 1 Ω. The previously found current stability with the DCV-mode would account for 100 mΩ. Also short integration times of the DMM are more sensitive to noise. The integration time of the DCV-DMMs was 1 ms, where the OHMF-DMM integrates the signal for 200 ms.

The offset translates to an increase of source current of 50 nA. This is significantly more than the found stability of 1 nA in 68 % of the time when measuring in the 10 kΩ-range. The offset can be caused by drift in, assumed to be constant, source current or shunt resistance. It is also possible the power generated by the multimeter depends somewhat on the applied circuit load.

The OHMF-method resulted in a resistance value of 9999.54 Ω ± 0.31 Ω ($k = 2$). The DCV-method combined with a shunt resulted in a resistance value of 9997.35 Ω ± 0.35 Ω ($k = 2$). These methods were compared using the EN-test. For this test, the found averages, Type A and Type B uncertainties were used. The test yielded a result value of 4.7, which indicates the DCV-method to be rejected, which is expected, as the measurement data with error bars do not overlap.

4.4 Effective power dissipation

Thermistor self-heat has been measured with the OCOMP setting both on- and off. This data was used to compare the plotted discrete differential equation mentioned in chapter 3.4. Figure 14 shows the plot of the measurement data and the discrete differential equation (19).

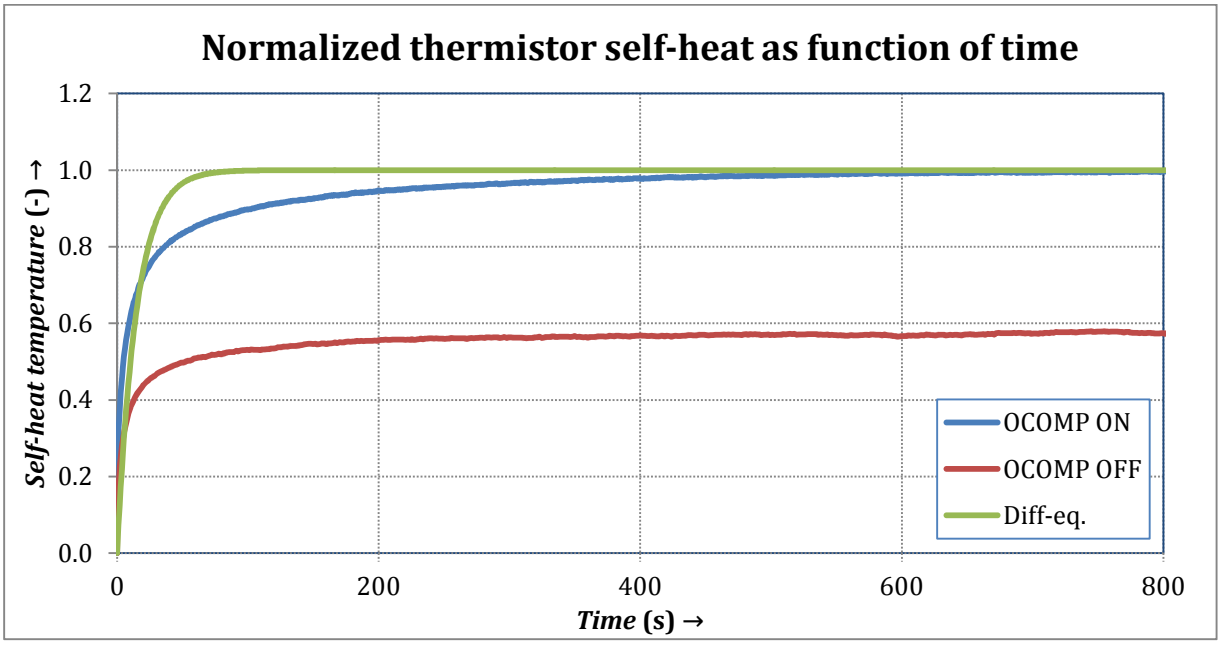

Figure 14 The plot of the normalized self-heat in time. The red and blue lines are plotted measurement data. The green line represents a theoretical fit

The blue- and red lines are the data of the thermistor self-heat with OCOMP and without OCOMP, respectively. The green line is the plot of equation (19). Some constants like the heat transfer of the thermistor to water and the mass and heat capacity of the thermistor are relatively unknown; therefore these have been altered to find the best fit possible to the measurement data. Equation (19) appears to be a poor fit to the measurement data. The differential equation should be solved with the power already as a time-dependent factor and fitted again to the measurement data. Unfortunately this could not be achieved as the resulting equation is complex and would take too much time to be able to fit it with the measurement data.

4.5 Uncertainty analysis

The mentioned values for the uncertainty provided with the results are determined in this chapter. The discussed uncertainty in chapter 3.6 gives the basis for the values found in the uncertainty tables provided in this chapter.

4.5.1 Uncertainty in current stability

The current stability was measured in two different ways. One was directly measuring the current and the other involved measuring a voltage over a resistor/shunt. The uncertainty of the former exists of the statistical, Type A, uncertainty and the Type B specified uncertainties of the DMM. The table below shows the found values for the current stability using the DCI method. The results using both methods are presented in Table 3.

Table 3 An overview of the results of the current stability measurement

Measurement function	Number of samples measured	Measured average	Standard deviation	Standard uncertainty of the mean
DCI	21499	97.5334 µA	3.37878 nA	15.7160 pA
DCV	4517	0.975134 V	10.2534 µV	2.26996 nV
OHMF	4517	9997.98 Ω	8.70362 mΩ	1.92686 µΩ

The corresponding uncertainties are discussed per measurement method, i.e. DCI-mode and shunt-method (DCV over the shunt resistor). The contributions to the uncertainty will be discussed and their values explained. Table 4 contains the uncertainty budget of the DCI-mode.

Table 4 The uncertainty budget of the current stability measurement using the DCI method

Symbol	Description	uncertainty		Distribution	Divider	u_x (ppm)
DCI-mode						
I	Calibration	1.5	ppm	Normal	1.00	1.5
I	Accuracy of reading	25	ppm	Rectangular	1.73	14
I	Accuracy of range	8.0	ppm	Rectangular	1.73	4.6
I	Temperature coefficient reading	0.2	ppm	Rectangular	1.73	0.12
I	Temperature coefficient range	0.1	ppm	Rectangular	1.73	0.06
I	Noise	20	ppm	Rectangular	1.73	12
I	Gain	3	ppm	Rectangular	1.73	1.7
I	Time-axis	1	ppm	Rectangular	1.73	0.58
I	Reading DMM	1	aA	Rectangular	1.73	$5.8 \cdot 10^{-9}$
I	Standard deviation of the mean (Type A)	0.16	pA	Normal	1.00	$1.6 \cdot 10^{-3}$
				Expanded uncertainty for k = 1		19
				Expanded uncertainty for k = 2		38

The column "uncertainty" presents the uncertainty obtained from measurements or literature. These have to be normalized for coverage and made relative. The final column contains the relative uncertainty with coverage of 68%. These uncertainties are added according to equation (26).

The calibration uncertainty is obtained from the calibration. A measurement offset is found and corrected for to obtain more accurate values. The uncertainty in this measurement with k=2 is determined to be 3 ppm. To be able to compare the results, it is divided by 2 to obtain the k = 1 value.

The reading accuracy is a measure for the stability of the DMM. The two year stability according to the specifications of the DMM (DMM_manual, 2012, p. 287) has been used. This is also the frequency the DMMs are usually calibrated with. The corresponding uncertainty consists of two parts, uncertainties relative to the reading and the range. The values for the reading and range are already incorporated in the third column.

The temperature coefficients of the DMM are given in ppm $\cdot°C^{-1}$. The DMMs are constantly kept on to keep them warmed up at all times. The variation in ambient air temperature during a measurement in the laboratory is ±0.1°C. The corresponding values have been adjusted to this temperature change.

The noise and gain errors are given in ppm of range and reading, respectively. A graph is provided, in Figure 15, which contains these errors as function of the integration time. The RMS-noise error has to be multiplied by a factor depending on the range of the measurement function. Of the used ranges, this only applies to the 1 V DCV-range, with a multiplication factor of 2.

The time axis errors are described in chapter 3.6.1 and determined to be, at most, 1 ppm.

The reading error in the DMM is the last digit which is unsure due to rounding errors. However, the used DMMs provide readings of 15 digits through the GPIB-bus. This read error is found to be negligible with all used measurement functions with this measurement set-up.

The standard deviation of the mean is the standard uncertainty found in the statistics. This is the Type A uncertainty and is accounted for in Table 3.

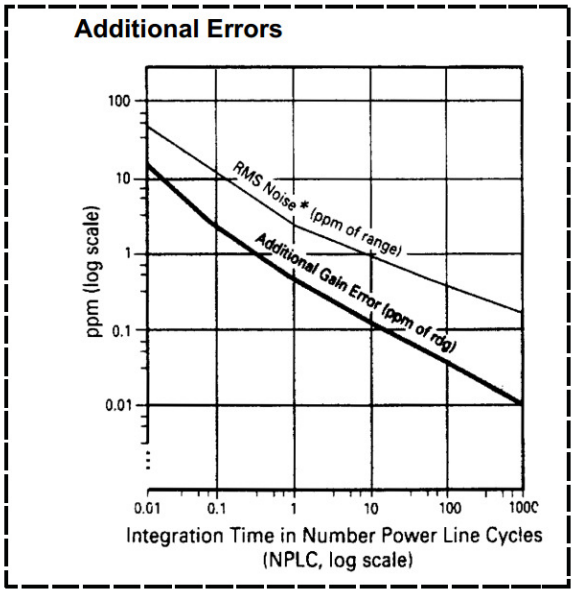

Figure 15 The noise and gain errors of the DMMs DCI-mode as function of the integration time

The last rows contain the total uncertainties with coverage of $k = 1$ and $k = 2$. The corresponding level of confidence of the uncertainty is 68% and 98% respectively.

The found value for the current using the DCI-mode is 97.5334 μA ± $3.7 \cdot 10^{-3}$ μA, with $k = 2$.

4.5.2 Determining the uncertainty of current stability with the DCV-mode combined with a shunt

Because the current was indirectly determined in this method, the sensitivity of the uncertainty to a change in voltage or resistance needs to be evaluated using partial differentiation:

$$u_I^2 = \left(\frac{\partial I}{\partial V} \cdot u_V\right)^2 + \left(\frac{\partial I}{\partial R} \cdot u_R\right)^2 \tag{29}$$

u_I	the uncertainty in the current	[I]
u_V	the uncertainty in the voltage	[V]
u_R	the uncertainty in the resistance	[Ω]

Inserting equation (21) and evaluating the partial differentiations gives

$$u_I^2 = \left(\frac{1}{R} \cdot u_V\right)^2 + \left(\frac{V}{R^2} \cdot u_R\right)^2 \tag{30}$$

Dividing by the current gives the relative uncertainty in the measured current

$$\left(\frac{u_I}{I}\right)^2 = \left(\frac{1}{\frac{R}{V}} \cdot u_V\right)^2 + \left(\frac{\frac{V}{R^2}}{\frac{V}{R}} \cdot u_R\right)^2 = \left(\frac{u_V}{V}\right)^2 + \left(\frac{u_R}{R}\right)^2 \quad (31)$$

This form always appears when determining the relative uncertainty of a linear product function. This means that the sensitivity is 1 and no additional correction is needed to be able to compare the uncertainties of the resistance and voltage measurements. Table 5 shows the evaluated uncertainties of the current measurement using the voltage over the shunt and its resistance value.

Table 5 The uncertainty budget of the current measurement with the DCV-mode combined with a shunt

Symbol	Description	uncertainty		Distribution	Divider	u_x (ppm)
DCV-mode						
V	Calibration	1	ppm	Normal	1.00	1
V	Accuracy of reading	10	ppm	Rectangular	1.73	5.8
V	Accuracy of range	0.3	ppm	Rectangular	1.73	0.17
V	Temperature coefficient reading	0.015	ppm	Rectangular	1.73	$1 \cdot 10^{-3}$
V	Temperature coefficient range	0.01	ppm	Rectangular	1.73	$1 \cdot 10^{-3}$
V	Noise	1.5	ppm	Rectangular	1.73	0.87
V	Gain	5	ppm	Rectangular	1.73	2.9
V	Linearity of reading	0.3	ppm	Rectangular	1.73	0.17
V	Linearity of range	0.1	ppm	Rectangular	1.73	0.06
V	Time-axis	1	ppm	Rectangular	1.73	0.58
V	Reading DMM	1	fV	Rectangular	1.73	$5.8 \cdot 10^{-10}$
V	Standard deviation of the mean (Type A)	2.27	nV	Normal	1.73	$2.3 \cdot 10^{-3}$
OHMF-mode						
R	Calibration	13	ppm	Normal	1.00	13
R	Accuracy of reading	15	ppm	Rectangular	1.73	8.7
R	Accuracy of range	1	ppm	Rectangular	1.73	0.58
R	Temperature coefficient reading	0.1	ppm	Rectangular	1.73	0.06
R	Temperature coefficient range	0.01	ppm	Rectangular	1.73	$1 \cdot 10^{-3}$
R	Noise	2	ppm	Rectangular	1.73	1.2
R	Gain	2	ppm	Rectangular	1.73	1.2
R	Time-axis	1	ppm	Rectangular	1.73	0.58
R	Reading DMM	0.1	pΩ	Rectangular	1.73	$5.8 \cdot 10^{-8}$
R	Standard deviation of the mean (Type A)	1.93	μΩ	Normal	1.00	$1.9 \cdot 10^{-4}$
				Expanded uncertainty for k=1		17
				Expanded uncertainty for k=2		34

The uncertainties provided in this table are obtained the same way as in Table 4. There is one uncertainty added for the DCV-mode, which is the transfer linearity of the voltmeter. The uncertainties are given in ppm of reading and range. The uncertainties found in the table above have their corresponding values incorporated.

The obtained value using the DCV-mode is 97.5308 µA ± $3.3 \cdot 10^{-3}$ µA, with (k = 2).

The obtained average values and uncertainties were used to compare the measurement methods using an EN-test. These values are provided in Table 6.

Current measurement (DCI, DCV over a shunt)	Average (µA)	U_I(µA) k=1	En-test
DCI	97.5334	$3.7 \cdot 10^{-3}$	0.53
DCV with shunt	97.5308	$3.3 \cdot 10^{-3}$	

Table 6 The EN-test results of current measurement; the DCI-method versus the DCV-method

Current measurement (DCI, DCV over a shunt)	Average (µA)	U_I(µA) k=1	En-test
DCI	97.5334	$3.7 \cdot 10^{-3}$	0.53
DCV with shunt	97.5308	$3.3 \cdot 10^{-3}$	

The EN-test value is found to below the criterion of an EN-test value equal or smaller than two. This means that the measuring of DCV over a shunt is an accepted method to measure current. Because of lower uncertainties, this method will be used in future current measurements.

4.5.3 Uncertainty in the resistance verification

The resistance verification was done by using three DMMs where one was measuring resistance over a two parallel connected, stable, 20 kΩ resistors (R2 and R3). The second DMM was measuring the voltage over the same resistors and the third measured the voltage over a shunt placed in series with the reference resistors. The uncertainty table for R2 and R3 is presented in found in Appendix VI Full uncertainty budgets. Because the two parallel resistors have about the same value as the shunt and the current passing through them is the same, the two DCV-DMMs are measuring in the same range. Their uncertainty budgets amount to the same as in Table 5, except for any Type A contributions, although these tend to be negligible compared to the type B uncertainty. Table 7 contains the uncertainty budget of the OHMF-measurement with the parallel resistors. The full uncertainty budget of the two DCV-DMMs combined with a shunt is provided in Appendix VI Full uncertainty budgets.

Table 7 The uncertainty budget of the OHMF-measurement of the parallel connected resistors, R2 and R3

Symbol	Description	uncertainty		Distribution	Divider	u_x (ppm)
OHMF-mode						
R	Calibration	13	ppm	Normal	1.00	13
R	Accuracy of reading	15	ppm	Rectangular	1.73	8.7
R	Accuracy of range	1	ppm	Rectangular	1.73	0.58
R	Temperature coefficient reading	0.1	ppm	Rectangular	1.73	0.06
R	Temperature coefficient range	10	ppb	Rectangular	1.73	0.01
R	Noise	2	ppm	Rectangular	1.73	1.2
R	Gain	2	ppm	Rectangular	1.73	1.2
R	Time-axis	1	ppm	Rectangular	1.73	0.6

R	Reading DMM	0.1	pΩ	Rectangular	1.73	$5.8 \cdot 10^{-12}$
R	Standard deviation of the mean (Type A)	1.93	μΩ	Normal	1.00	$1.9 \cdot 10^{-4}$
				Expanded uncertainty for k = 1		15
				Expanded uncertainty for k = 2		31

The obtained value for the combined resistance of the two parallel resistors is 9999.54 Ω ± 0.31 Ω, with k = 2. Below is a summarized version of the uncertainty budget of the method using two DCV-DMMs.

Table 8 Summarized uncertainty table of the two DCV-DMMs combined with a shunt

Symbol	Description	uncertainty		Distribution	Divider	u_x (ppm)
DCV-mode (sense of OHMF)						
V	Expanded uncertainty	6.6	ppm	Normal	1.00	6.6
DCV-mode (sense of shunt)						
V	Calibration	6.6	ppm	Normal	1.00	6.6
shunt						
R	Obtained Type B uncertainty	15	ppm	Normal	1.00	15
				Expanded uncertainty for k = 1		18
				Expanded uncertainty for k = 2		35

This method resulted in a resistance value of 9998.36 Ω ± 0.35 Ω, with k = 2.

These methods were compared using an EN-test. This used data is displayed in Table 9

Table 9 EN-test of the OHMF-DMM method versus two DCV-DMMs combined with a shunt

R2||R3 (DCV,OHMF)	Average (Ω)	Type A uncertainty (Ω)	Type B uncertainty (Ω)	UR2||R3(Ω)	En-test
R2||R3 OHMF	9999.54	0.00	0.31	0.31	4.7
R2||R3 DCV, DCV	9997.35	0.00	0.35	0.35	

The EN-test value is larger than the set criterion of 2. The DCV-method with a shunt is rejected on this basis.

5 Conclusion and recommendations

The goal of the assignment is to find an accurate description of thermistor self-heating. A custom measurement program was needed to be developed to achieve this. The development was more time consuming than was estimated at first. This resulted in the lack of an accurate, complete, description of thermistor self-heating. However, a lot was learned about the possibilities and limitations of the Agilent 3458A opt. 002 DMM. The following aspects were studied:

- The precise course of the resistance during the heating of the thermistors due to the source current (using sampling techniques).
- Optimizing the DMM measuring circuit with respect to signal to noise ratio and reduction of possible interference.
- Determination of the precise timing of the integration time on the heating curve.
- Determination of the effective dissipated power comparing a constant source current versus a square-wave source current.
- The effects of variation in the settings of the digital multimeter used to measure the thermistors
- Confirming the resistance value using two extra digital multimeters to validate both current and voltage.

Experimenting with the sampling sequence led to the discovery that the part of the self-heating curve that is integrated to be used in the resistance measurement, is actually the first, and steepest part of the heating curve.

Signal interference was detected in the measurements. This noise was reduced by grounding the Lauda cooler the same as the DMMs and switching the guards of the DMMs to “open”. The signal to noise ratio was increased by a factor 34.

Thermistor resistance is measured in the OHMF-mode of the DMM. This cancels out interference in the source current using voltage ratios. The fluctuations in power dissipation by the thermistor however, are not canceled out. The source current was measured to determine its stability using two methods. The current was measured directly using the DMM’s DCI-mode. This resulted in a source current value of 97.5334 μA ± $3.7 \cdot 10^{-3}$ μA, with $k = 2$. The current was also measured by measuring the voltage over a known resistor, R1 (10 kΩ). This method yielded a source current value of 97.5308 μA ± $3.3 \cdot 10^{-3}$ μA, with $k = 2$. Standard deviations of 35 · μA/A for the DCI-mode and 11 μA/A for the DCV-mode were obtained in these measurements. Which indicates the current to fluctuate within 1 nA in 68 % of the time when measuring in the 10 kΩ-range. The two methods were validated using the EN-test. The result of this test resulted in an EN-test value of 0.53, which satisfies the criterion of an EN-test value equal or smaller than two. Therefore, the DCV-method was used for later current measurements.

The OCOMP setting of the DMM directly influences the self-heat curve, as this periodically disables and enables the source current. The self-heat curve was approximated using a discrete form of the differential equation for the self-heat. This curve did not match the plotted measurement data for thermistor self-heat. A possible explanation for this can be a steep temperature gradient in the water due to its stillness.

The method of measuring thermistor resistance was validated by using two reference resistors, R2 (20 kΩ) and R3 (20 kΩ), connected parallel measuring the current through- and the voltage over these resistors. The current was measured by placing a shunt, R1 (10 kΩ), in series with these resistors. The voltage over R1 and its resistance are used to calculate the current through the shunt, and thus the resistors. The OHMF-method measuring the parallel resistors resulted in a value for the resistance of 9999.54 Ω ± 0.31 Ω ($k = 2$). The DCV-method combined with a shunt resulted in a resistance value of 9997.35 Ω ± 0.35 Ω ($k = 2$). These methods were compared using the EN-test. For this test, the found

averages, Type A and Type B uncertainties were used. The test yielded a result value of 4.7, which indicates the DCV-method to be rejected, which is expected, as the measurement data with error bars do not overlap. The plotted data shows a stable graph of the resistance obtained through the OHMF-method. The DCV-method in combination with a shunt shows an offset in average resistance value and a significant standard deviation. The offset can be caused that long-term drift of the shunt, which has not been characterized and the impact of a larger load on the current source. The large standard deviation is unlikely to be caused by instability in the source current alone. But can be caused by the noise of short integration times used to measure the voltage, 1 ms with the DCV-mode versus 200 ms in the OHMF-mode.

Some settings are required for the measurement program to function properly. The most important settings are discussed individually below.

DISP ON: Although this adds a delay to the measurement sequence, it prevents an unknown extra reading to appear in the first measurement.

MEM FIFO: This outputs the data chronologically. MEM LIFO outputs the readings of a measurement in reversed order. Which in inconvenient in continuous measurements, and MEM OFF outputs only the last value. In the used triggering settings, this value is the AZERO reading with source current disabled, which holds no useful information.

OFORMAT DINT: Output the data in the double integer format. This format requires the least amount of bits, while retaining maximum resolution.

END OFF: Unlike ASCII, the output format DINT does not contain its own line-feed or carriage-return bits. This command ensures the readings are kept separate.

NRDGS, EVENT: Sets the number of readings that will be made once the trigger is armed and the trigger event is satisfied. Possible events include, but are not limited to: “EXT”, the EXT TRIG input, “AUTO”, as soon as the controller requests data or “TIMER”, with a specified time interval between the start of two readings.

TARM: During initialization the trigger is unarmed, or on “hold”. The DMMs can be initialized and will wait until both the trigger arm event, as the trigger events are satisfied. Clicking the “Measure drift” button sends the trigger arm command and the DMM starts measuring as soon as the trigger arm- and the trigger events are satisfied. Giving the OHMF-DMM a single trigger arm was considered. When each DMM is read out, the OHMF-DMM would receive another single trigger. This makes the speed of the program direct how fast the measurements are done. It was believed the measurement program would not be fast enough to process all the data and slowing the measurement sequence down to the speed of the program could be beneficial. However, the system with the single triggers somehow caused the DCV-DMMs to not do any readings.

5.1 Recommendations

A general recommendation for the limitation of the self-heat is the use of a stable external current source which is able to provide a lower current to the thermistor. Using a 10 kΩ thermistor, the power dissipated by the thermistor with a 10 μA current source would drop with a factor 100 considering the OHMF-mode, which would drive a 100 μA through the thermistor. This would apply a voltage of 100 mV over the thermistor, which could be accurately measured using the 100 mV range of the DCV-mode of the DMM, which is approximately only a few ppm’s less accurate than the DCV-mode in the 1 V range, but more accurate than the OHMF-mode according to the DMM specifications.

The defect in the effective power dissipation may be caused by convection. This had been considered negligible, but may cause the heat of the thermistor to be transported away, thus dampening the self-heating. An expression for the effective dissipated power including convection may provide a better fit to the measurement data.

The data received from the DMM contains a total of four readings, two if which are AZERO measurements. The other two are OCOMP readings and used to calculate the true reading value. The AZERO readings are processed internally and pose no use in the data received by a DCV-DMM. An alteration in triggering may result in the correct reading being outputted by the MEM OFF command. This way every reading received is relevant.

There are still uncertainties about the exact measurement sequence. The user's manual of the DMM seems to contradict itself concerning the OCOMP setting. The manual states on page 209 that the low OCOMP reading is done before the high OCOMP reading, while the same manual states the opposite on page 62. When actively correcting the self-heat for the part of the self-heat curve that is integrated for OHMF-measurements, it is important to be sure about this measurement sequence.

5.1.1 Resistance verification recommendations

During the resistance verification measurements only one 1 ms sample was taken with the DCV-DMMs for each reading of the OHMF-DMM. With the used settings, the OHMF-DMM integrates this signal for 200 ms. With AZERO on, the total integration time of the DCV-DMMs can be increased to about 75 ms, when other delays are minimal (DISP OFF). The time the ADC is integrating can be increased by increasing the number of 1 ms samples, but is best done by increasing the integration time itself as this decreases contributions of noise- and gain errors.

Considering measuring current with a shunt and the DCV-mode, the use of a resistor with lower resistance value as a shunt to minimize errors due to the input impedance is found to not be efficient. When using a shunt resistor of 500 Ω, the gain in a lower input impedance error would decrease to 1 ppm to 0.05 ppm. This traded off with a gain in errors due to measurement range which would increase by 3 ppm. This trend continues when using lower resistance shunts without altering the source current accordingly.

List of symbols

β	a material constant	[K]
δ	heat-transfer coefficient of the thermistor	[W/K]
ε	the correction factor for non-ideal blackbody radiators	[-]
σ	the Stefan-Boltzmann constant	[=5.670·10^{-8} W/m^2·K^4]
a	the half-width between the upper and lower limits	[-]
A	the surface area of the radiating object	[m^2]
B	an arbitrary physical quantity	[-]
C_p	the specific heat capacity of water at constant pressure	[=4207.5 J/kg·K]
C_{Th}	the heat capacity of the thermistor	[J/kg·K]
D_w	the absorbed dose in water	[J/kg]
E	energy	[J]
E_a	the absorbed energy by the water	[J]
F	an arbitrary physical quantity	[-]
G	an arbitrary physical quantity	[-]
H	the arbitrary physical quantity H dependent of F and G	[-]
I	the source current	[A]
I_{DUT}	the current through the resistor	[A]
$I_{X\mu A}$	the measuring current at X µA	[A]
k	the coverage factor	[-]
m	the mass of the thermistor	[kg]
m_w	the mass of the water absorbing the energy	[kg]
n	the number of samples taken	[-]
P	the dissipated power by the resistor	[W]
P_0	the total dissipated power by the thermistor with constantly applied current	[W]
P_1	the reference sample	[-]
P_2	the sample under test	[-]
P_{eff}	the effective dissipated power by the thermistor with OCOMP on	[W]
P_R	the emitted thermal energy by an object per second	[W]
$P_{\mathrm{X\mu A}}$	the power dissipated by the thermistor at a measuring current of X µA	[W]
R	the resistance of the thermistors	[Ω]
R_0	the thermistor resistance without an applied current	[Ω]
$R(T)$	the thermistor resistance as a function of temperature	[Ω]
$R_0(X\mu A)$	the thermistor resistance without measuring current extrapolated using X µA data	[Ω]
R_{DUT}	the calculated resistance	[Ω]
$R_{\mathrm{X\mu A}}$	the thermistor resistance at a measuring current of X µA	[Ω]
$R_{OCOMP\ on}$	the thermistor resistance at equilibrium with OCOMP on	[Ω]
$R_{OCOMP\ off}$	the thermistor resistance at equilibrium with OCOMP off	[Ω]

R_{shunt}	the resistance value of the shunt	[Ω]
s	the standard deviation of the sample	[-]
t	time	[s]
T_o	the absolute temperature of the object	[K]
T	the absolute temperature of the thermistor	[K]
ΔT	temperature difference between the water and the thermistor	[K]
$\Delta T_{SH}(t)$	the increment in temperature due to the self-heat effect as a function of time	[K]
ΔT_w	the change in temperature of the water	[K]
T_0	the absolute reference temperature	[K]
T_0	the thermistor temperature at *n=0*	[K]
T_c	the absolute temperature of the environment	[K]
t_n	the time at *n*	[s]
T_n	the thermistor temperature at *n*	[K]
T_{SH}	the temperature increment due to the self-heat effect	[K]
T_{Th}	the thermistor temperature	[K]
T_w	the temperature of the water	[K]
U	the expanded uncertainty	[-]
$u(A)$	the uncertainty in the arbitrary physical quantity A	[-]
$u(H)$	the uncertainty in the arbitrary physical quantity H dependent of F and G	[-]
$u(X)$	the uncertainty in the arbitrary physical quantity X dependent of F and G	[-]
u_c	the combined standard uncertainty	[-]
u_I	the uncertainty in the current	[I]
u_{P_1}	the standard uncertainty in P_1	[-]
u_{P_2}	the standard uncertainty in P_2	[-]
u_R	the uncertainty in the resistance	[Ω]
u_{rect}	the standard uncertainty of a rectangular uniform distribution	[-]
$u_{Type\ A}$	the Type A uncertainty of a sample	[-]
u_V	the uncertainty in the voltage	[V]
V	the measured voltage over the resistor	[V]
V_{DUT}	the voltage over the resistor	[A]
V_{shunt}	the voltage over the shunt	[V]
x	the EN-test result	[-]
X	the arbitrary physical quantity X	[-]

Appendix I: Graduation internship assignment

Below, the original internship assignment (in Dutch) is included.

Selfopwarmingseffecten van thermistoren in de VSL watercalorimeter bij toepassing van een commerciële DMM (Agilent 3458A opt. 002)

De Nederlandse primaire standaard voor geabsorbeerde dosis in water bij VSL is een watercalorimeter. In de watercalorimeter wordt ten gevolge van bestraling met externe bundels hoogenergetische röntgen- of gammastraling een temperatuursverandering gemeten waaruit de geabsorbeerde dosis in water wordt bepaald met behulp van de volgende vergelijking:

$$D_w = C_{p,w}\,\Delta T$$

Hierin is $C_{p,w}$ de soortelijke warmte van water bij constante druk, $C_{p,w}$ = 4207,5 J/kg/K en ΔT in K de gemeten temperatuursverandering als gevolg van de bestraling. Deze temperatuursverandering wordt gemeten in water bij een nominale temperatuur van 4 °C.

Een bestraling van 1 Gy, afgegeven in ca. ½ tot 1 minuut, resulteert in een temperatuursverandering van minder dan 240 µK. Deze temperatuursverandering dient met een standaarddeviatie van 1 % bepaald te worden, wat overeenkomt met temperatuur van 2,4 µK.

De temperatuursverandering ten gevolge van de bestraling wordt gemeten met twee NTC-elementen met afmetingen van ca. 0,35 mm ingebed in glazen buisjes met een buitendiameter van 0,7 mm, zogenaamde thermistoren. Deze thermistoren zijn aangesloten op een digitale multimeter, DMM, van het type Agilent 3458A opt. 002. Als gevolg van de meetstroom afkomstig van de DMM, die door de NTC-elementen loopt, wordt een vermogen gedissipeerd . Het gedissipeerde vermogen heeft als gevolg dat de thermistoren een ca. 20 - 60 mK hogere temperatuur hebben dan het omgevende medium, water. Tijdens een bestralingsrun verandert de weerstand van de thermistor en daarmee deze zogenaamde zelfopwarming.

De mate van verandering van zelfopwarming in relatie tot de temperatuursverandering van het omringende medium is afhankelijk van de instellingen van de DMM. Instellingen zoals 'auto zero', 'delay', 'offset compensatie' en het moment waarop de integratie plaatsvindt, hebben invloed op de zelfopwarming en de thermistor.

De afstudeeropdracht bestaat uit het modelleren van zelfopwarmingseffecten van de thermistoren in de watercalorimeter met Comsol MultiPhysics bij verschillende DMM instellingen en het verifiëren van de resultaten met de praktijk. Het uiteindelijke doel is te komen tot een toepasbare zelfopwarmingscorrectie met een bijbehorend onzekerheidsbudget.

Appendix II The determination of the heat-transfer coefficient, δ

(de Prez, 2007 (revised 2008)) The heat-transfer coefficient is a constant which describes the relation between the temperature increment of the thermistor relative to the medium in which it is placed, and the dissipated power in the thermistor. As mentioned in chapter 2.3.3, the value of δ depends of several variables, like: the used materials in the thermistor, the construction of the probe and the properties of the surrounding medium. Therefore δ has to be determined for each individual thermistor.

The value of δ under calibration conditions is determined by measuring the resistance of the thermistor while applying two different currents for each temperature. The different current, and thus, power applied over the thermistor is used, along with the measured change in resistance to extrapolate to a 0 A source current, which means, no self-heat. This is done using the equation below:

$$\left(\frac{dR}{dP}\right)=\frac{R_{5\mu A}-R_{10\mu A}}{P_{5\mu A}-P_{10\mu A}} \tag{32}$$

With:

$R_{X\mu A}$ the thermistor resistance at a measuring current of X µA [Ω]

$P_{X\mu A}$ the power dissipated by the thermistor at a measuring current of X µA [W]

Where:

$$P_{X\mu A}=I_{X\mu A}{}^{2}\cdot R_{X\mu A} \tag{33}$$

With:

$I_{X\mu A}$ the measuring current at X µA [A]

The thermistor resistance without the self-heat contribution can then be calculated using:

$$R_0\left(X\mu A\right)=R_{X\mu A}-\frac{dR}{dP}\cdot P_{X\mu A} \tag{34}$$

With:

$R_0\left(\mathrm{X\mu A}\right)$ the thermistor resistance without measuring current extrapolated using X µA data [Ω]

The found values for R_0 should match other found values for R_0 with different current, but only apply for the temperature that the measurements were done at. When R_0 is determined for enough values of T, the relation between R_0 and T can be fitted. From this fit, the thermistor calibration coefficients, which are needed for an accurate polynomial fit, can be determined. This leads to the determination of the sensitivity, S_0, at zero source current. This is done using the equation below:

$$\delta_{calibration}=\left(\left(\frac{dR}{dP}\right)\cdot\left(\frac{dT}{dR}\right)\right)^{-1}=\left(\left(\frac{dR}{dP}\right)_{calibration}\right)^{-1}\cdot R_0\cdot S_0 \tag{35}$$

The heat-transfer coefficient is independent of temperature, but other factors, which are not, may impede on the accuracy of this value. Multiple of these $\delta_{calibration}$ can be determined at different temperatures to get an average heat-transfer coefficient with one standard uncertainty.

Appendix III Used settings for DMM

There are more commands sent to the DMM to ensure the triggering and measurements are done at the correct timing and accuracy. The settings are used during several types of measurements that have not yet been mentioned in chapter 3.2.2 will be briefly explained to understand their function. The table below contains the used settings for the resistance verification measurement. The two DCV-DMMs (the middle and right initialization pane) contain the same settings because their function is the same.

Table 10 Used DMM settings for the resistance verification measurement

DMM1	DMM2	DMM2
RESET	RESET	RESET
PRESET DIG	PRESET DIG	PRESET DIG
MEM OFF	MEM FIFO	MEM FIFO
INBUF ON	INBUF ON	INBUF ON
MFORMAT DINT	MFORMAT DINT	MFORMAT DINT
OFORMAT DINT	OFORMAT DINT	OFORMAT DINT
END ALWAYS	END ALWAYS	END ALWAYS
OHMF 10000	DCV 1	DCV 1
OCOMP ON	;	;
AZERO ON	AZERO ON	AZERO ON
DELAY -1	DELAY -1	DELAY -1
NPLC 10	APER 1e-3	APER 1e-3
NDIG 10	NDIG 10	NDIG 10
;	TIMER 0.01	TIMER 0.01
NRDGS 1, AUTO	NRDGS 1, TIMER	NRDGS 1, TIMER
TRIG AUTO	TRIG EXT	TRIG EXT
TARM HOLD	TARM HOLD	TARM HOLD
EXTOUT APER, NEG	;	;
DISP ON	DISP ON	DISP ON
TARM AUTO	TARM AUTO	TARM AUTO

RESET: Resets the DMM to power-on settings without actually shutting down.

PRESET DIG: Sets the DMM to one of the presets with standard values for delay-, timer- and aperture- values. In this case the preset is for digitizing, giving accurate measurements.

INBUF ON: Enables the input buffer. The DMM stores the commands and executes them at once. This allows the controller to do other tasks while the DMM is initializing the settings.

MFORMAT DINT: Similar to OFORMAT, MFORMAT sets the format of the reading memory. This may differ from the OFORMAT, converting data types occurs between the reading memory and outputting the data.

OHMF/DCV: Sets the measurement function of the DMM along with the corresponding range.

DELAY -1: Sets the minimum delay between the trigger event and the first sample event.

NDIG 10: Sets the display resolution of the DMM. The "10" ensures maximal resolution is displayed.

NRDGS, EVENT: It sets the number of readings the DMM makes per EVENT. AUTO sets this to maximum. TIMER sets a certain time interval, or sample frequency, between measurements. The product of integration time and number of readings may not exceed the time defined by the TIMER command. The DMM will give a "TRIGGER TOO FAST" error and ignores all triggers until the readings are finished.

TRIG EVENT: Selects at what event the DMM triggers. AUTO triggers the DMM as soon as the controller requests data. "EXT" uses the EXT trig input of the DMM and triggers on the negative slope of a TTL-signal.

TARM HOLD: The trigger arm event. The DMM starts measuring when the trigger arm and the trigger event are satisfied. When the trigger arm event is set to HOLD the DMM cannot be triggered.

TARM AUTO: This arms the trigger as soon as the controller requests data. This command is executed separately from the others because the DMMs start measuring as soon as the trigger is armed and the trigger event is satisfied. For synchronization, the OHMF-is sent the "TARM AUTO" last.

Appendix IV Writing a custom measurement program

To be able to monitor the resistance of the thermistor a new program was written to be able to retrieve data fast enough to be able to map the course of the resistance. Shortly hereafter, the program was updated to command and retrieve data from two, and later three, DMMs. The DMMs make a set number of readings upon being triggered. When the measurements are made, the DMMs "arm" command returns to "hold". The program processes the readings of all DMMs and arms the DMMs when the readings are fully processed. This makes the measurement program run continuously. At each of these loop iterations a timestamp is given to accompany the readings. This way the readings can be plotted in the correct timeframe.

The program sends commands to the DMMs one at a time. To make sure all DMMs make readings at the same time, the two DCV-DMMs are triggered externally to the aperture waveform of the OHMF-DMM. The DCV-DMMs are armed first and will start measurements when their trigger events are satisfied. Their trigger is the activity of the ADC of the OHMF-DMM. This DMM is armed lastly so that the two DCV-DMMs are 'waiting' on the measurement of the OHMF-DMM, which is triggered automatically.

The new program is capable of faster readings because it uses the reading memory of the DMM. The DMM is capable of storing measurements in the reading memory and emptying this in one time. The reading rate of 25 kB/s can then be used optimally. The DMM can output readings in several formats including, but not limited to, ASCII, SINT (single integer) and DINT (double integer). The output in ASCII is the easiest to read by a program because the readings are sent as a string which is the value of the reading. ASCII however is not the most efficient output format, as there are addresses reserved for all characters in the ASCII table and only the numbers are used for the readings. Each ASCII reading takes 16-bits of data, including the "end of line" and "line feed" characters (DMM_manual, 2012, p. 98). The output formats SINT and DINT send integer values and take up only 2- and 4-bits of data, respectively. The reading values are compressed so they can be expressed as integer values. The integer values have to be multiplied by a scaling factor to retrieve the original reading value. This scaling factor is based on the measurement function, range and integration time.(DMM_manual, 2012, p. 188).

Appendix V Calibration certificates

Below are the tables which contain parts of the calibration certificates of the used DMMs

Table 11 Certificate of Agilent 3458A opt 002. Serial number: US28029799; certificate number: 3351760

Range (V)	Presented value (V)	Measured value (V)	Uncertainty in measured value (μV/V)
1	0.970 000 0	0.970 005 6	2
1	0.980 000 0	0.980 005 7	2
1	0.990 000 0	0.990 005 7	2
Range (kΩ)	Presented value (kΩ)	Measured value (kΩ)	Uncertainty in measured value (μΩ/Ω)
10	1.900 00	1.899 99	100
10	10.000 00	9.999 93	25
100	19.000 0	19.000 0	30
100	100.000 0	99.999 6	10

Table 12 Certificate of Agilent 3458A opt 002. Serial number: US28029739 certificate number: 3351761

Range (V)	Presented value (V)	Measured value (V)	Uncertainty in measured value (μV/V)
1	0.970 000 0	0.970 005 0	2
1	0.980 000 0	0.980 005 0	2
1	0.990 000 0	0.990 005 1	2
Range (kΩ)	Presented value (kΩ)	Measured value (kΩ)	Uncertainty in measured value (μΩ/Ω)
10	1.900 00	1.900 01	100
10	10.000 00	10.000 00	25
100	19.000 0	19.000 1	30
100	100.000 0	100.000 2	10

Table 13 Certificate of HP 3458A opt 002. Serial number: 2823A13955; certificate number: 3351986

Range (V)	Presented value (V)	Measured value (V)	Uncertainty in measured value (μV/V)
1	1.000 000 0	0.999 999 6	2
1	0.500 000 0	0.499 999 8	2
1	0.200 000 0	0.200 000 0	6

Table 14 Certificate of HP 3458A opt 002. Serial number: US28029739; certificate number: 3352107

Range (μA)	Presented value (μA)	Measured value (μA)	Uncertainty in measured value (μA/A)
10	10.000 00	9.999 93	12
100	100.000 0	100.000 1	3

Appendix VI Full uncertainty budgets

Uncertainty budget of R2

Symbol	Description	uncertainty		Distribution	Divider	u_x (ppm)
OHMF-mode						
R	Calibration	13	ppm	Normal	1.00	13
R	Accuracy of reading	15	ppm	Rectangular	1.73	8.7
R	Accuracy of range	5	ppm	Rectangular	1.73	2.9
R	Temperature coefficient reading	0.1	ppm	Rectangular	1.73	0.06
R	Temperature coefficient range	0.05	ppm	Rectangular	1.73	0.03
R	Noise	10	ppm	Rectangular	1.73	5.8
R	Gain	2	ppm	Rectangular	1.73	1.2
R	Time-axis	1	ppm	Rectangular	1.73	0.56
R	Reading DMM	0.1	pΩ	Rectangular	1.73	$1 \cdot 10^{-11}$
R	Standard deviation of the mean (Type A)	1.3	mΩ	Normal	1.00	0.07
				Expanded uncertainty for k=1		16
				Expanded uncertainty for k=2		33

Because R2 and R3 have a small difference in resistance, all uncertainties originating from specifications or ranges are the same. The difference in uncertainty for these resistors is in the statistical uncertainty. These only differ within 0.1‰ from each other. With the rounding applied in the table above, the table for either will be identical to the other.

Table 15 Full uncertainty budget of the resistance verification measurement using the DCV-method combined with a shunt

Symbol	Description	uncertainty		Distribution	Divider	u_x (ppm)
DCV-mode (sense of OHMF)						
V	Expanded uncertainty	1	ppm	Normal	1.00	1
V	Accuracy of reading	10	ppm	Rectangular	1.73	5.8
V	Accuracy of range	0.3	ppm	Rectangular	1.73	0.17
V	Temperature coefficient reading	0.02	ppm	Rectangular	1.73	0.01
V	Temperature coefficient range	0.01	ppm	Rectangular	1.73	0.01
V	Noise	1.5	ppm	Rectangular	1.73	0.87
V	Gain	5	ppm	Rectangular	1.73	2.9
V	Linearity of range	0.1	ppm	Rectangular	1.73	0.06
V	Linearity of reading	0.3	ppm	Rectangular	1.73	0.17
V	Time-axis	1	ppm	Rectangular	1.73	0.58
V	Reading DMM	1	fV	Rectangular	1.73	$1 \cdot 10^{-9}$
V	Standard deviation of the mean (Type A)	0.16	µV	Normal	1.00	0.16
DCV-mode (sense of shunt)						
V	Calibration	1	ppm	Normal	1.00	1
V	Accuracy of reading	10	ppm	Rectangular	1.73	5.8
V	Accuracy of range	0.3	ppm	Rectangular	1.73	0.17
V	Temperature coefficient reading	0.02	ppm	Rectangular	1.73	0.01
V	Temperature coefficient range	0.01	ppm	Rectangular	1.73	0.01
V	Noise	1.5	ppm	Rectangular	1.73	0.87
V	Gain	5	ppm	Rectangular	1.73	2.9
V	Linearity of range	0.1	ppm	Rectangular	1.73	0.06
V	Linearity of reading	0.3	ppm	Rectangular	1.73	0.17
V	Time-axis	1	ppm	Rectangular	1.73	0.58
V	Reading DMM	1	fV	Rectangular	1.73	$1 \cdot 10^{-10}$
V	Standard deviation of the mean (Type A)	0.40	µV	Normal	1.00	0.41
Shunt resistor						
R	Obtained Type B uncertainty	15	ppm	Normal	1.00	15
				Expanded uncertainty for k = 1		18
				Expanded uncertainty for k = 2		35

Bibliography

BIPM. (n.d.). *Standard for absorbed dose to water in Co-60 gamma radiation*. Retrieved from www.bipm.org: http://www.bipm.org/en/scientific/ionizing/dosimetry/Co60/absorbed_dose.html

Cen, J. (2011). *Self-heat effect of thermistors for absorbed dose measurements.* Delft: VSL/NMI.

Chatfield, C. (1996). *Statistics for technology, A course in applied statistics.* Bristol: Chapman and Hall.

de Prez, L. A. (2007 (revised 2008)). *De NMi standaard voor geabsorbeerde dosis in water in hoogenergetische fotonenstraling.* Delft: NMI, VSL.

DMM_manual. (2012). Agilent Technologies 3458A Multimeter User's Guide. Loveland, USA: Agilent Technologies Incorporated.

Giancoli, D. C. (2009). *Natuurkunde.* Amsterdam: Pearson Education Benelux bv.

internal communication. (n.d.).

Kessler, C., Allisy-Roberts, P. J., de Prez, L. A., & de Pooter, J. A. (2009). *Comparison of the standards for absorbed dose to water of the VSL and the BIPM for Co-60 gamma rays.* Sèvres/Delft: BIPM/VSL.

Microchiptechnologies. (2010). Retrieved from www.microchiptechno.com: http://www.microchiptechno.com/ntc_thermistors.php

Seuntjens, J. (1991). *Comparative study of ion chamber dosimetry and water calorimetry in medium energy x-ray beams.* Gent: Rijksuniversiteit Gent.

Swerlein, R. L. (1989). Precision AC Voltage Measurements Using Digital Sampling Techniques. *Hewlett-Packard Journal issue 1989 nr.4* , p. 15-21.